Variational Image Inpainting

TONY F. CHAN
University of California, Los Angeles

AND

JIANHONG (JACKIE) SHEN
University of Minnesota

Dedicated to Gil Strang on the occasion of his 70th birthday.

Abstract

Inpainting is an image interpolation problem with broad applications in image and vision analysis. Described in the current expository paper are our recent efforts in developing universal inpainting models based on the Bayesian and variational principles. Discussed in detail are several variational inpainting models built upon geometric image models, the associated Euler-Lagrange PDEs and their geometric and dynamic interpretations, as well as effective computational approaches. Novel efforts are then made to further extend this systematic variational framework to the inpainting of oscillatory textures, interpolation of missing wavelet coefficients as in the wireless transmission of JPEG2000 images, as well as light-adapted inpainting schemes motivated by Weber's law in visual perception. All these efforts lead to the conclusion that unlike many familiar image processors such as denoising, segmentation, and compression, the performance of a variational/Bayesian inpainting scheme *much more crucially* depends on whether the image prior model well resolves the spatial coupling (or geometric correlation) of image features. As a highlight, we show that the Besov image models appear to be less interesting for image inpainting in the wavelet domain, highly contrary to their significant roles in thresholding-based denoising and compression. Thus geometry is the single most important keyword throughout this paper.

Contents

Communications on Pure and Applied Mathematics, Vol. LVIII, 0579–0619 (2005)

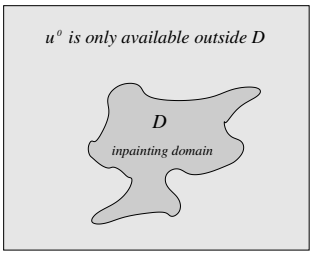

FIGURE 1.1. For a typical inpainting problem, the image is missing on an inpainting domain D, and the available part $u^0\big|_{D^c}$ is often noisy. D can have *many* connected components with arbitrary shapes and sizes.

1 Introduction: Bayesian and Model-Based Inpainting

The word *inpainting* is an artistic synonym for "image interpolation," as initially circulated among museum restoration artists, who manually remove cracks from degraded ancient paintings by following as faithfully as possible the intention of their original creators [38, 90]. This beautiful term was first introduced into digital image processing in the work of Bertalmio et al. [9]. A mathematical illustration is depicted in Figure 1.1.

Image interpolation is such a classical topic in image and vision analysis that there are numerous existing works. In the engineering literature, for example, one finds the following samples from a large pool: image interpolation [4, 57, 58], image replacement [50, 92], error concealment [52, 59] in communications technology, and image editing in the contour domain [37]. In mathematical image and vision analysis (MIVA), image interpolation has also been studied in the remarkable works of Nitzberg, Mumford, and Shiota for segmentation with depth [75], Masnou and Morel for completion of level lines [65], as well as Caselles, Morel, and Sbert for axiomatic interpolation using second-order partial differential equations (PDEs) [15].

The recent wave of interest in digital inpainting was largely inspired by the work of Bertalmio, Sapiro, Caselles, and Ballester [9], where the authors proposed an intriguing third-order inpainting PDE. Ever since, digital inpainting models and techniques have witnessed broad applications in image processing, vision analysis, and the movie industry. Recent examples include: automatic scratch removal in digital photos and old films [9, 20], text erasing [6, 9, 20, 21], special effects such as object

disappearance and wire removal for movie production [9, 21], zooming and super-resolution [6, 20, 61, 62, 88], lossy perceptual image coding [20], decomposition-based image interpolation [10, 89], landmark-based inpainting [53], removal of the laser dazzling effect [27], and so on.

The approaches for inpainting-related problems are as diversified as the applications are, ranging from the nonlinear filtering method, the wavelets and spectral method, to the statistical method (especially for textures).

The most recent approach to image inpainting is based on the PDE method and the calculus of variations, and can be classified into two categories. The first class is based on the simulation of micro-inpainting mechanisms and includes the axiomatic approach from local specifications [15], the transport process [9] (the first high-order PDE model), the diffusion process [21], and their combination based on the Navier-Stokes equation in fluid dynamics and axiomatic modeling [8, 22]. The second category includes all variational models simulating the unique macro-inpainting mechanism: "best guess," or the Bayesian framework [44, 56, 70]. The latter includes the total variation model [19, 20, 79, 80], the functionalized elastica model [18, 65], the value-and-direction joint model [6], the active contour model based on Mumford and Shah's segmentation [88], and the inpainting scheme based on the Mumford-Shah-Euler image model [39].

The current expository paper surveys and further explores this latter category. The main goal is to develop a systematic approach and mathematical foundation for all these previously scattered works so that the current work can serve as a fresh starting point rather than a concluding chapter for further future research on this challenging but significant topic. In particular, we shall reveal and highlight the characteristic significance of *geometric* ingredients in variational inpainting models.

Compared with other methods, the Bayesian/variational approach is more universal in terms of applicability, better structured in terms of model developing, and more flexible in terms of model updating and multitask modeling. The current work should be able to illustrate these attractive features thoroughly.

The philosophy behind Bayesian inpainting is quite accessible (see Figure 1.1): the way we human inpainters inpaint an incomplete picture relies mostly on two factors—how we read the existing part of the picture $u^0|_{\Omega\setminus D}$ (i.e., *data model*), and what class of images we believe the original complete and clean picture u belongs to (i.e., *image prior model*). For example, if it is known that we are inpainting an image of a kitchen with tomatoes, peppers, and apples, we have the a priori preference of smooth shapes and the green and red colors. In the Bayesian language, a balanced optimal guess is to maximize the a posteriori probability $\text{Prob}(u \mid u^0)$ (MAP)

$$\text{Prob}(u \mid u^0, D) = \frac{\text{Prob}(u^0 \mid u, D) \cdot \text{Prob}(u \mid D)}{\text{Prob}(u^0 \mid D)}. \tag{1.1}$$

Once an observation u^0 and its missing domain D are given, the denominator is a fixed constant. On the other hand, since the missing mechanism is often independent of the image content, $\text{Prob}(u \mid D) = \text{Prob}(u)$. Thus we are to maximize the product of the data probability and the image probability.

For inpainting, the data model is usually simple, as illustrated in Figure 1.1: the available part $u^0|_{\Omega\setminus D}$ is the restriction on $\Omega \setminus D$ of a degraded version of the underlying true image u,

$$u^0\big|_{\Omega\setminus D} = (K[u] + n)\big|_{\Omega\setminus D},$$

where n denotes an additive white noise and K a possible blur or point-spreading function (PSF). For simplicity, we shall only work with the blurfree case when K is the identity operator. (For examples with Gaussian PSF or motion blur, see the authors' work in [23].)

On the other hand, since there is no data available on the inpainting domain D, the task of reconstructing the image on D falls solely on the image model. This makes a good image model more crucial for inpainting than any other classical restoration problems such as denoising, deblurring, and segmentation [20, 39].

Image models can be learned from image data banks based on filtering, parametric or nonparametric estimation, and the maximum entropy principle (see Zhu, Wu, and Mumford [93, 94] for examples). Such a statistical approach is especially important for inpainting or synthesizing images with rich textures [50, 92].

On the other hand, in most inpainting problems, the inpainting domain often "erases" some perceptually important *geometric* information of the image. Incomplete or broken edges are typical examples. To reconstruct geometry, it is necessary that the image model well resolves the geometry a priori. Most conventional probabilistic models lack such a feature. Fortunately, geometry-motivated "energy" forms do exist in the literature. Well-known examples include the TV (total variation) model of Rudin, Osher, and Fatemi [80] and the object-edge model of Mumford and Shah [73]. The link between probabilistic image models and such geometric image models, as Mumford pointed out [70], is formally made through Gibbs' formula in statistical mechanics [45]:

$$\text{Prob}(u) = \frac{1}{Z}\exp(-\beta E[u]),$$

where $E[u]$ is the energy of u (e.g., the total variation of u), β the inverse absolute temperature, and Z the partition function. (Working with energy also frees one from laboring on the definability of the partition function Z, which is generally a highly nontrivial mathematical issue. Interested readers are directed to the remarkable recent work of Mumford and Gidas [72].) The Bayesian formula (1.1) is expressed in the energy form by

$$E[u \mid u^0, D] = E[u^0 \mid u, D] + E[u] + \text{const},$$

where the constant can be dropped safely as far as energy minimization is concerned. The above view has also been emphasized in our recent two expository articles in the *Notices AMS* and *SIAM News* [25, 82].

The current paper is organized as follows:

In Section 2, for the first time in the literature, we propose a rigorous and universal definition of the inpainting problem, as well as make intriguing connections to several more familiar problems in the other areas of mathematics.

Section 3 starts with an axiomatic approach for curve models, preparing for the crucial modeling of *image priors* to be incorporated into variational inpainting schemes. The latter half of the section explains two universal approaches for constructing geometric image models from curve models:

(1) through direct functionalization via level sets and
(2) by having a curve model embedded as an edge model in the object-edge free-boundary image model.

These approaches unify the four geometric image models appearing in the recent inpainting literature:

(1) the BV (bounded variation) image model (via the TV (total variation) Radon measure) of Rudin, Osher, and Fatemi [79, 80], first applied to inpainting modeling by Chan and Shen [20]
(2) the functionalized elastica image model as proposed and studied by Masnou and Morel [65], and Chan, Kang, and Shen [18];
(3) the Mumford-Shah image model [73] applied to inpainting by Tsai, Yezzi, and Willsky [88], Chan and Shen [20], and Esedoglu and Shen [39]; and
(4) the Mumford-Shah-Euler image model designed for image inpainting by Esedoglu and Shen [39].

Section 4 describes all the recent inpainting schemes based on these geometric image models. We discuss the associated Euler-Lagrange PDEs, their geometric as well as dynamic meaning, and robust ways of numerical implementation.

Section 5 improves the preceding variational inpainting models by taking into account one fundamental feature of human visual perception: light adaptivity quantified by Weber's law in psychology, psychophysics, and retinal physiology. This work follows the recent papers by Shen [83] and Shen and Jung [84] on the important roles played by Weber's law in image and vision analysis. In addition, the new variational models are better justified in the framework of Tikhonov regularization theory than the Bayesian rationale, in contrast to all the other models in the current paper.

In Section 6, we study variational interpolation models for images with missing wavelet coefficients. We argue that the conventional notion of Besov image priors, which have contributed a great deal to the rigorous analysis of wavelet-based algorithms such as compression and denoising [16, 32, 33, 36], becomes surprisingly handicapped for image interpolation in the wavelet domain. Consequently,

we propose variational inpainting models that combine both geometric image priors on the pixel domain and the available information on the wavelet domain. This section shows that while wavelet diagonalization is advantageous for denoising and compression, the resulting lack of spatial correlations or coupling causes it to malfunction for inpainting. Inpainting is the extension of existing information into mission domains, for which spatial correlations (of both short range and long range) are crucial.

In Section 7, we discuss a variational *texture* inpainting model based on Yves Meyer's recent texture model [66] and its numerical approximation and implementation by Vese and Osher [89]. Our analysis again highlights the subtle difference between inpainting and the other classical image processing tasks such as denoising and segmentation. As in the preceding section, we conclude that a successful variational/Bayesian inpainting scheme always demands image or texture models that have geometry or spatial correlations explicitly built in.

A brief conclusion and some open problems are written into Section 8.

Throughout the paper, Ω denotes the entire image domain, D the missing inpainting domain, u^0 the observed image that is only available on the complement $\Omega \setminus D$, and u the targeted inpainting restoration. The standardized symbols ∇, $\nabla\cdot$, and Δ represent the gradient, divergence, and Laplacian operators, respectively. For any multivariable function or functional $F(X, Y)$, the symbol $F(X \mid Y)$ still means $F(X, Y)$, but emphasizing that Y is fixed as known. This is to imitate the symbol of conditional probability or expectation appearing in the Bayesian formula (but without probabilistic normalization).

Due to the substantial variational/PDE contents of the current paper, for readers from computer science, information and communication sciences, electrical or biomedical engineering, or other applied sciences, we suggest as references the two recent monographs on variational/PDE methods in image processing [5, 81], the expository paper on this subject co-authored by the authors [25], as well as the new book by the two authors to be published by the Society for Industrial and Applied Mathematics (SIAM) in early 2005 [24].

2 Mathematical Formulation and Background of Inpainting

Although most inpainting tasks discussed hereafter are mainly interpolation problems directly on pixel domains, it is still helpful to first develop a unified or abstract view on the nature of the inpainting problem.

Let $\mathcal{U}$ denote a target class of images whose structures are to be specified later, and let

$$T : \mathcal{U} \to \Phi, \quad u \to \phi = T[u],$$

be a linear or nonlinear operator that transforms $\mathcal{U}$ to another suitable data space Φ. We shall call T the *observable* operator.

DEFINITION 2.1 (Lossy Observable) An observable T is said to be *lossy* if and only if one of the following holds:

(1) $\ker(T) = T^{-1}(0)$ contains nonzero images, when $\mathcal{U}$ and T are both linear; or
(2) T is not injective, i.e., there exist two distinct images $u, v \in \mathcal{U}$ such that $T[u] = T[v]$, when $\mathcal{U}$ or T is nonlinear; or
(3) for some proper complexity measure H, one has $H(T[u]) < H(u)$, when $(\mathcal{U}, \mu)$ is a random ensemble defined by the probability distribution μ, and u treated as a random field. (For example, H could be the entropy measure or Kolmogrov's complexity [29].)

Concerning the last scenario, in information theory, when H is the entropy measure under base 2, $H(u)$ is often called the bit length of u. Thus for example, for a typical binary image u of 1000 by 1000 whose spatial patterns are unknown, one needs $H(u) = 1{,}000{,}000$ bits to send the information. After applying a square downsampling of factor 10 [87], the downsampled image ϕ is only 100 by 100 and $H(\phi)$ drops down to $10,000$. It is intuitively clear that ϕ loses about 99% of the information of u due to the lossy downsampling process.

DEFINITION 2.2 (Inpainting) Given a lossy observable T on an image class $\mathcal{U}$, *inpainting* is to reconstruct u from its observable $\phi = T[u]$.

Due to the lossy nature, inpainting is clearly an ill-posed inverse problem, which makes the Bayesian view stated above more pertinent and powerful.

EXAMPLE 1 (A Noninpainting Problem) Let $\mathcal{U} = L^2(\mathbb{R}^2)$ denote all square integrable images, and consider the observable T defined for some fixed $\tau > 0$ by

$$T : u \to \phi = T[u] = v(x, \tau), \quad x = (x_1, x_2) \in \mathbb{R}^2,$$

where for general $t \geq 0$, $v(x, t)$ denotes the solution to the heat equation

$$v_t = \frac{\sigma^2}{2} \Delta v, \quad v(x, 0) = u(x).$$

Then in the Fourier domain (with frequency variable denoted by $\omega \in \mathbb{R}^2$),

$$\hat{\phi}(\omega) = \exp(-c\omega^2) \cdot \hat{u}(\omega) \quad \text{for some positive constant } c = c(\sigma, \tau).$$

Thus the observable T is not lossy, though the inversion $u = T^{-1}[\phi]$ amounts to inverting the diffusion process and is notoriously unstable. In particular, to restore u from $\phi = v(x, \tau)$ is *not* an inpainting problem by our definition. In fact, if the above diffusion equation to some extent approximates the atmospheric scattering of light, then to recover u from ϕ is called the *deblurring* problem in astronomy or remote sensoring [24].

EXAMPLE 2 (BVP vs. Inpainting) Let Ω be a bounded Lipschitz domain in $\mathbb{R}^2$, and $\mathcal{U} = H^1(\Omega)$ all Sobolev images. Let the observable T be the boundary trace operator

$$\phi = T[u] = \partial_\Omega u := u\big|_{\partial\Omega}.$$

Clearly T is lossy, and recovering u from ϕ is therefore an inpainting problem by our definition. With proper differential constraints, such as the harmonic equation $\Delta u = 0$ or the Poisson equation $\Delta u = f$ on Ω, the inpainting process then simply becomes a boundary value problem (BVP). In [20], the authors first made such connections and developed rigorous error analysis for the resultant inpainting processes (see also the recent work by Chan and Kang [17]).

EXAMPLE 3 (MSP vs. Inpainting) A special BVP is the *minimum surface problem* (MSP) [48, 74]. For an MSP, assume that the image class is Sobolev, $\mathcal{U} = W^{1,1}(\Omega)$, and that $\phi = T[u]$ is still the boundary trace operator. An MSP is to reconstruct (or inpaint) u (or its graph) from its prescribed boundary configuration ϕ based on the criterion of minimum area,

$$\min_{u:T[u]=\phi} \mathcal{A}(u, \Omega) = \int_\Omega \sqrt{1 + |\nabla u|^2}\, dx.$$

For noisefree images, the TV (total variation) inpainting model of Chan and Shen [20] and its regularized computation are closely related to such MSPs. TV was first introduced into image processing by Rudin, Osher, and Fatemi [80].

EXAMPLE 4 (Shannon's Sampling Theorem vs. Inpainting) Consider one dimension, for example. Let $\mathcal{U} = L^2(\mathbb{R}^1)$ denote the class of square integrable signals, and $\Gamma \subset \mathbb{R}^1$ any Lebesgue-measurable subset. Define the observable operator T to be Γ-sampling

$$\phi = T[u] = u\big|_\Gamma = \{u(x) \mid x \in \Gamma\}.$$

Then as long as the Lebesgue measure $|\Gamma^c| = |\mathbb{R}^1 - \Gamma| > 0$, the observable T is lossy in L^2. On the other hand, suppose the image class is

$$\mathcal{U}_\pi = \{u \in L^2 \mid \operatorname{supp} \hat{u} \subseteq [-\pi, \pi]\},$$

the class of L^2-signals (whose Fourier transforms are) band-limited to $[-\pi, \pi]$. Then the celebrated *Shannon's sampling theorem* claims that if $\Gamma \supseteq \mathbb{Z}$ contains all integers, then $\phi = T[u]$ defined above is *not* lossy at all, and perfect reconstruction can be achieved for any $u \in \mathcal{U}_\pi$ by [25, 31]:

$$u(x) = \sum_{n \in \mathbb{Z}} \phi(n) \operatorname{sinc}(x - n), \quad \operatorname{sinc}(x) = \frac{\sin \pi x}{\pi x}.$$

Otherwise, suppose $\Gamma = 2\mathbb{Z}$ contains only all even integers. Then $\phi = T[u]$ defined above becomes lossy on $\mathcal{U}_\pi$, and the reconstruction of u from ϕ becomes an inpainting problem. The recent work by Smale and Zhou [85] further explores this line from the viewpoint of mathematical learning theory.

EXAMPLE 5 (Inpainting Markov Random Fields) Let $(\Omega, \mathcal{N})$ be a graph supported on a node set Ω (or a pixel domain) and with topology specified by the neighborhood system $\mathcal{N}$ [12]. For any node (or pixel) $\alpha \in \Omega$, $N_\alpha \in \mathcal{N}$ specifies all its neighbors. Given three sets of pixels $A, B, \Gamma \subseteq \Omega$, A and B are said to be *separated* by Γ if any connected path from some $a \in A$ to some $b \in B$ must intersect Γ.

A random field u (with probability distribution $p(u)$) on $(\Omega, \mathcal{N})$ is said to be Markovian with respect to the local topology $\mathcal{N}$ if for any $A, B \subseteq \Omega$ and any set Γ that separates them,

$$p(u_A, u_B \mid u_\Gamma) = p(u_A \mid u_\Gamma) p(u_B \mid u_\Gamma),$$

where u_A denotes the marginal of u restricted on A. That is, u_A and u_B are independent given the information of u_Γ. For convenience, we have adopted the same symbol u_A to denote both the random field and a particular single sample.

For any proper subset of pixels $A \subset \Omega$, let $\phi = T[u] = u_A$ denote the marginal of a Markov random field u. Then by the entropy formula [29],

$$H(u) = H(\phi, u_{A^c}) = H(\phi) + H(u_{A^c} \mid \phi), \quad A^c = \Omega \setminus A.$$

Generically, as long as u_{A^c} cannot be *deterministically* constructed given the data u_A, the second term of conditional entropy (or bit length) must be positive. Thus generically one must have $H(\phi) < H(u)$, and T is lossy according to the previous definition.

Now define

$$\Gamma = \partial A = \{\beta \in A^c \mid \beta \in N_\alpha \text{ for some } \alpha \in A\}.$$

Then for any $B \subseteq A^c$, A and B must be separated by ∂A. In particular,

$$p(u_A \mid u_{\partial A}, u_B) = p(u_A \mid u_{\partial A}).$$

Therefore if one defines $v = (u_A, u_{\partial A})$ and $\psi = u_{\partial A}$, then to infer (or inpaint) v given ψ can be seen as the stochastic version of the boundary value problem in Example 2. We refer to Geman and Geman [44] and Mumford [71] for deeper exploration into Markov random fields.

We hope that all the above examples have adequately motivated the inpainting problem against a broader background of mathematics. As the title suggests, this paper will only focus on deterministic inpainting problems and their variational approaches. The single most important keyword in our models is *geometry*.

3 Geometric Image Models

3.1 Curve Models

Geometry plays a crucial role in visual perception and image understanding, including classification and pattern recognition. The most important geometry for image analysis resides within edges. From David Marr's classical work on primal sketch [64] to David Donoho's geometric wavelet analysis [35], edges always stay in the heart of many issues: image coding and compression, image restoration, and segmentation and tracking, just to name a few.

Therefore it is of paramount importance to understand how to mathematically model edges and curves.

From the Bayesian point of view, this is to establish a probability distribution Prob(Γ) over "all" curves. An example that instantly comes to mind is Brownian motion and its associated Wiener measure [55]. The problem is that Brownian paths are parametrized curves (by "time") and are even almost surely nowhere differentiable. For image analysis, however, edges are intrinsic (one-dimensional) manifolds and their regularity is an important visual cue.

According to the previously stated Gibbs' formulation, we are also to look for a suitable energy form $e[\Gamma]$. It is always convenient to start first with its digital version.

In digital image processing, Freeman's *chain coding* [43] is a popular data structure for representing object borders and edges. The underlying idea is to represent a one-dimensional curve Γ by a chain of ordered sample points

$$x_0, x_1, \ldots, x_N,$$

dense enough to ensure reasonable approximation. Working directly with such chains of finite length, one needs to define appropriate energy forms

$$e[x_0, x_1, \ldots, x_N].$$

In what follows, guided by several natural axioms, we shall construct two of the most useful planar curve models: the length energy and Euler's elastica energy.

AXIOM 1 (Euclidean Invariance) Let $Q \in O(2)$ (conventionally called a rotation, though including all reflections), and $c \in \mathbb{R}^2$ be an arbitrary point. Euclidean invariance consists of two parts: the rotational invariance

$$e[Qx_0, \ldots, Qx_N] = e[x_0, \ldots, x_N]$$

and the translation invariance

$$e[x_0 + c, \ldots, x_N + c] = e[x_0, \ldots, x_N].$$

AXIOM 2 (Reversal Invariance) This variance requires that

$$e[x_0, \ldots, x_N] = e[x_N, \ldots, x_0],$$

which means that the energy does not depend on the orientation of the curve.

AXIOM 3 (p-Point Accumulation ($p = 2, 3, \ldots$)) This is fundamentally a rule on the *local* interaction or coupling of pixels. A p-point accumulative energy satisfies the accumulation law

$$e[x_0, \ldots, x_n, x_{n+1}] = e[x_0, \ldots, x_n] + e[x_{n-p+2}, \ldots, x_{n+1}]$$

for all $n \geq p - 2$. Through cascading, one easily establishes the following proposition:

PROPOSITION 3.1 *Suppose e is p-point accumulative. Then for any $N \geq p - 1$,*

$$e[x_0, \ldots, x_N] = \sum_{n=0}^{N-p+1} e[x_n, \ldots, x_{n+p-1}]$$

Thus, for example, a two-point accumulative energy must be in the form of

$$e[x_0, \ldots, x_N] = e[x_0, x_1] + e[x_1, x_2] + \cdots + e[x_{N-1}, x_N],$$

and a three-point accumulative energy satisfies

$$e[x_0, \ldots, x_N] = e[x_0, x_1, x_2] + e[x_1, x_2, x_3] + \cdots + e[x_{N-2}, x_{N-1}, x_N].$$

Generally, a p-point accumulative energy e is completely determined by its fundamental form

$$e[x_0, \ldots, x_{p-1}].$$

In what follows, we study the cases of $p = 2$ and $p = 3$.

Two-Point Accumulative Energy and the Length

PROPOSITION 3.2 *A Euclidean invariant two-point accumulative energy must be in the form of*

$$e[x_0, \ldots, x_N] = \sum_{n=0}^{N-1} f(|x_{n+1} - x_n|)$$

for some nonnegative function $f(s)$.

PROOF: It suffices to show that

$$e[x_0, x_1] = f(|x_1 - x_0|).$$

Translation invariance leads to

$$e[x_0, x_1] = e[0, x_1 - x_0] = F(x_1 - x_0)$$

with $F(x) = e[0, x]$. Then rotational invariance further implies that

$$F(Qx) \equiv F(x), \quad Q \in O(2),\ x \in \mathbb{R}^2.$$

Thus if we define $f(s) = F((s, 0))$, then $F(x) = f(|x|)$. □

If, in addition, we impose linear additivity, whereby for any $\alpha \in (0, 1)$ and $x_1 = \alpha x_0 + (1 - \alpha)x_2$,

$$e[x_0, x_2] = e[x_0, x_1] + e[x_1, x_2],$$

then it is easy to show that the energy is unique up to a multiplicative constant.

THEOREM 3.3 *A continuous and Euclidean invariant two-point accumulative energy e with linear additivity must be the* length *energy, i.e.,*

$$e[x_0, \ldots, x_N] = c \sum_{n=0}^{N-1} |x_n - x_{n+1}|$$

for some fixed positive constant c.

For a summable curve Γ, as $N \to \infty$ and the sampling size

$$\max_{0 \le n \le N-1} |x_n - x_{n+1}|$$

tends to 0, such digital energy converges to the length.

Three-Point Accumulative Energy and the Curvature

To determine the fundamental form $e[x_0, x_1, x_2]$, first recall Frobenius' classical theorem [13]. The three points x_0, x_1, x_2 live in $\mathbb{R}^6 = \mathbb{R}^2 \times \mathbb{R}^2 \times \mathbb{R}^2$, and the dimension of a Euclidean orbit is 3 : 1 from the rotation group, and 2 from the translation group. Therefore, Frobenius' theorem applied to the Euclidean invariance gives the following:

PROPOSITION 3.4 *One can find exactly three independent joint invariants, I_1, I_2, and I_3, such that $e[x_0, x_1, x_2]$ is a function of them.*

Define

$$a = |x_1 - x_0|, \quad b = |x_2 - x_1|, \quad c = |x_2 - x_0|.$$

Then the ordered triple (a, b, c) is apparently Euclidean invariant, and two chains $[x_0, x_1, x_2]$ and $[y_0, y_1, y_2]$ are Euclidean congruent if and only if they share the same (a, b, c). Thus there must exist a nonnegative function $F(a, b, c)$ such that

$$e[x_0, x_1, x_2] = F(a, b, c).$$

Define the two elementary symmetric functions of a and b:

$$A_1 = \frac{a+b}{2} \quad \text{and} \quad B_1 = ab. \tag{3.1}$$

The reversal invariance implies the symmetry of F with respect to a and b. Thus e has to be a function of A_1, B_1, and c:

$$e[x_0, x_1, x_2] = f(A_1, B_1, c).$$

Let s denote the half-perimeter of the triangle (x_1, x_2, x_3):

$$s = A_1 + \frac{c}{2},$$

and Δ its area:

$$\Delta = \sqrt{s(s-a)(s-b)(s-c)} = \sqrt{s(s-c)(s^2 - 2A_1 s + B_1)}.$$

Then one can define the digital curvature at x_1 [11, 13, 14] by

$$\kappa_1 = 4\frac{\Delta}{B_1 c} = \frac{\sin\theta_1}{c/2}, \tag{3.2}$$

where θ_1 is the angle facing the side $[x_0, x_2]$. It is shown by Calabi, Olver, and Tannenbaum [14] that for a generic smooth curve and a fixed point x_1 on it, as $a, b \to 0$,

$$\kappa_1 = \kappa(x_1) + O(|b-a|) + O(a^2 + b^2),$$

where $\kappa(x_1)$ is the absolute curvature at x_1.

Now it is easy to see that κ_1, A_1, B_1 is a complete set of joint invariants for both the Euclidean and reversal invariances, and

$$e[x_0, x_1, x_2] = g(\kappa_1, A_1, B_1).$$

Therefore, we have proven the following:

THEOREM 3.5 *A three-point accumulative energy e with both Euclidean and reversal invariances must be in the form of*

$$e[x_0, \ldots, x_N] = \sum_{n=1}^{N-1} g(\kappa_n, A_n, B_n).$$

Further notice that, as the sampling size $a, b = O(h)$, $h \to 0$ at a fixed point $x_1 \in \Gamma$,

$$\kappa_1 = O(1), \quad A_1 = O(h), \quad B_1 = O(h^2).$$

If one assumes that g is a smooth function of its arguments, Taylor expansion with respect to the infinitesimals A_1 and B_1 leads to

$$g(\kappa_1, A_1, B_1) = \phi(\kappa_1)A_1 + \psi(\kappa_1)B_1 + \cdots \tag{3.3}$$

for some functions $\phi, \psi, \ldots$. In linear integration theory, by neglecting all the nonlinear high-order infinitesimals, one ends up with

$$g(\kappa_1, A_1, B_1) = \phi(\kappa_1)A_1.$$

Therefore we have derived the following:

COROLLARY 3.6 *Suppose* Γ *is a regular* C^2 *curve, and the size of its chain coding approximation* $[x_0, \ldots x_N]$,

$$h = \max_{0 \le n \le N-1} |x_n - x_{n+1}|$$

tends to 0. *In addition, following Theorem* 3.5, *assume that g is at least* C^1. *Then as far as the continuum limit is concerned, there is only one class of three-point accumulative energy with both Euclidean and reversal invariances, which is given by*

$$e[x_0, \ldots, x_N] = \sum_{n=1}^{N-1} \phi(\kappa_n)A_n, \tag{3.4}$$

with ϕ *defined as in* (3.3), *the digital arc length element A's as in* (3.1), *and the digital curvature* κ*'s as in* (3.2). *And as* $h \to 0$, *it converges to*

$$e[\Gamma] = \int_\Gamma \phi(\kappa) ds,$$

where ds is the arc length element along Γ.

Notice that the C^2 assumption on Γ is necessary for the curvature feature κ to be well-defined and continuous. The C^1 assumption on g justifies the Taylor expansion in (3.3), as well as the definability and continuity of $\phi(\kappa)$, so that the Riemann sum in (3.4) indeed converges to $e[\Gamma]$.

As an example, if one takes $\phi(\kappa) = \alpha + \beta\kappa^2$ for two fixed weights α and β, the resulting energy is called the elastica energy [69], which was first studied by Euler in modeling the shape of a torsion-free thin rod in 1744. If $\beta = 0$, the elastica energy degenerates to the length energy.

3.2 Image Models via Functionalizing Curve Models

Once a curve model $e[\Gamma]$ is established, it can be "lifted" to an image model by direct functionalization and the level-set approach.

Let $u(x)$ be an image defined on a domain $\Omega \subset \mathbb{R}^2$. For the moment, assume that u is smooth so that almost surely for each gray value λ, the level set

$$\Gamma_\lambda = \{x \in \Omega : u(x) = \lambda\}$$

is a smooth one-dimensional manifold. (Such values are said to be *regular* in differential topology [67], and the set of all regular values are well-known to be open and dense.) Let $w(\lambda)$ be an appropriate nonnegative weight function. Then based on a given *curve* model $e[\Gamma]$, one can construct an *image* model:

$$E[u] = \int_{-\infty}^{\infty} e[\Gamma_\lambda] w(\lambda) d\lambda.$$

For example, $w(\lambda)$ could be set to 1 to reflect human perceptual sensitivity. This is justified as follows: Consider a bundle of level sets whose gray values are concentrated over $[\lambda, \lambda + \Delta\lambda]$. If $\Delta\lambda$ is small, then the image appears smooth over the region made of these level sets and is thus less sensitive to perception. The energy assigned to such bundles should be small accordingly. On the other hand, if $\Delta\lambda$ is large, for example in the situation when the bundle contains a sharply transitory edge, then the level sets carry important visual information and the associated energy should be large as well. Therefore, the Lebesgue measure $d\lambda$ is already perceptually motivated and $w(\lambda)$ could indeed be set to 1, which we shall assume in what follows.[1]

Suppose we take the length energy in Theorem 3.3 as the curve model; then the resulting image model

$$E[u] = \int_{-\infty}^{\infty} \text{length}(\Gamma_\lambda) d\lambda$$

is exactly Rudin-Osher-Fatemi's TV (total variation) model [79, 80]:

$$E[u] = \int_\Omega |\nabla u| dx.$$

This is because for a smooth image u, along any level set Γ_λ,

$$d\lambda = |\nabla u| d\sigma, \quad \text{length}(\Gamma_\lambda) = \int_{\Gamma_\lambda} ds,$$

[1] On the other hand, if u and λ are understood as light intensity values (or photon counts in the quantum setting), then the recent works by Shen [83] and Shen and Jung [84] show that it is also desirable to take $w(\lambda) = 1/\lambda$ in the spirit of a well-known visual perception rule called *Weber's law*. Section 4 will also briefly revisit this interesting subject.

with ds and $d\sigma$ denoting the arc lengths of the level sets and their dual gradient flows, which are orthogonal to each other. In particular,

$$ds\, d\sigma = dx = dx_1\, dx_2$$

is the area element, and the lifted energy is indeed the total variation measure:

$$E[u] = \int_{-\infty}^{\infty} \int_{\Gamma_\lambda} |\nabla u| d\sigma\, ds = \int_{\Omega} |\nabla u| dx.$$

The above derivation is in a formal level and can be rigorously established based on the theory of BV (bounded variation) functions [48], where the length of a level set is replaced by the perimeter of its associated region, and the Sobolev norm by the TV Radon measure. Then the lifting process gives precisely the famous co-area formula of Fleming and Rishel [42] and De Giorgi [46, 48].

Similarly, suppose we take the curvature curve model in Corollary 3.6; then the lifted image model becomes

$$E[u] = \int_{\Omega} \phi(\kappa) |\nabla u| dx = \int_{\Omega} \phi\left(\left| \nabla \cdot \left[\frac{\nabla u}{|\nabla u|} \right] \right| \right) |\nabla u| dx. \tag{3.5}$$

Especially, if $\phi(s) = \alpha + \beta s^2$, it is called the "elastica image model" by Chan, Kang, and Shen [18, 65].

Rigorous theoretical study of the second-order geometric energy (3.5) turns out to be much more challenging than the total variation measure and the co-area formula. De Giorgi conjectured that the elastica model is some sort of singular limit of geometric measures, and Bellettini, Dal Maso, and Paolini of De Giorgi's school have indeed conducted some remarkable preliminary analysis [7].

3.3 Image Models with Embedded Edge Models

The second approach to construct image models from curve models is based on the object-edge free-boundary (or mixture) model, as proposed by Mumford and Shah [73] and Geman and Geman [44]. In such image models, the curve model is embedded to weigh the energy from the edges, i.e., abrupt jumps in images.

For example, the classical Mumford-Shah image model employs the length curve model:

$$E[u, \Gamma] = \int_{\Omega \setminus \Gamma} |\nabla u|^2\, dx + \alpha\, \text{length}(\Gamma).$$

Here Γ denotes edge collection. Unlike the TV image model, once the singular set Γ is singled out, Sobolev smoothness can be legally imposed for the rest of the image domain.

The Mumford-Shah image model has been very successful in image segmentation and denoising. For image inpainting, as Esedoglu and Shen discussed in [39], it is intrinsically insufficient for faithful interpolation. Therefore a new image

model called Mumford-Shah-Euler is proposed in [39] based on the elastica curve model

$$E[u, \Gamma] = \int_{\Omega\setminus\Gamma} |\nabla u|^2\, dx + \int_{\Gamma} (\alpha + \beta\kappa^2) ds,$$

where the elastica energy is embedded to enforce the second-order geometric regularity of the edges.

Likewise in the functionalization approach, the Mumford-Shah model could be properly studied in the framework of *special functions with bounded variations* (SBV), as beautifully done by De Giorgi, Carriero, and Leaci [47], and Dal Maso, Morel, and Solimini [30], and later by many others as well. The "edge" set Γ is then replaced by the weaker jump set of an SBV image, and accordingly its length energy by the one-dimensional Hausdorff measure $\mathcal{H}^1$. On the other hand, rigorous study on the Mumford-Shah-Euler image model encounters the very same difficulty as in the elastica image model. The main challenge is again rooted in the lack of proper functional spaces that have the second-order geometry (i.e., the curvature) intrinsically built in. The spaces of BV and SBV are only of first order.

Nevertheless in practice, with suitable numerical conditioning and approximation techniques, all these free-boundary geometric image models are quite effective in numerous real applications. We now discuss how to carry out inpainting based on these image models.

4 Geometric Variational Inpainting and Euler-Lagrange PDEs

In this section, we survey all the recent inpainting schemes based on the geometric image models mentioned above. We shall describe the PDE forms for all the variational models, the underlying geometric or dynamic meaning, and their digital realization based on the numerical PDE method. Digital examples are demonstrated for each inpainting scheme.

4.1 The TV Inpainting

In [20], we first touched on the Bayesian idea for the inpainting problem as an alternative to the PDE approach invented by Bertalmio et al. [9]. The image model employed in [20] is the well-known Rudin-Osher-Fatemi's BV image model, as first proposed for the denoising and deblurring application [79, 80].

The TV inpainting model is to minimize the posterior energy

$$E_{\mathrm{tv}}[u \mid u^0, D] = \int_{\Omega} |\nabla u| dx + \frac{\lambda}{2} \int_{\Omega\setminus D} (u - u^0)^2\, dx. \tag{4.1}$$

(The first term should have been written more rigorously as $\int_{\Omega} |Du|$, the TV Radon measure. But we have used the symbol D to denote a generic inpainting domain.) Define the masked Lagrange multiplier

$$\lambda_D(x) = \lambda \cdot 1_{\Omega\setminus D}(x). \tag{4.2}$$

Then the steepest-descent equation for the energy is

$$\frac{\partial u}{\partial t} = \nabla \cdot \left[\frac{\nabla u}{|\nabla u|} \right] + \lambda_D(x)(u^0 - u), \tag{4.3}$$

which is a diffusion-reaction type of nonlinear equation. To justify the drop of the boundary integral coming from the variational process, the associated boundary condition along $\partial\Omega$ has to be adiabatic: $\partial u/\partial \vec{\nu} = 0$, where $\vec{\nu}$ denotes the normal direction of the boundary.

The diffusion is anisotropic to respect sharp edges as in the Perona-Malik diffusion [78] since the diffusivity coefficient $1/|\nabla u|$ becomes small where u has sharp jumps. The reaction term has u^0 as its attractor to keep the solution close to the given noisy image. But notice that on the inpainting domain D, the equation is a pure diffusion process, which of course originates from the BV image model.

In [18], the existence of a minimizer of E_{tv} in the BV space is established based on the direct method of calculus of variation. The uniqueness, however, is generally not guaranteed. An example is given in [18]. Nonuniqueness, from the vision point of view, reflects the uncertainty of human visual perception in certain situations, and thus should not be viewed as a flaw in the model. In the Bayesian framework of statistical decision making, the nonuniqueness often results from the multimodality of the decision function or the a posteriori probability.

For the digital realization of model (4.3), the degenerate diffusion coefficient $1/|\nabla u|$ is always conditioned to

$$\frac{1}{|\nabla u|_a}, \quad |\nabla u|_a = \sqrt{a^2 + |\nabla u|^2},$$

for some small positive constant a. From the energy point of view, it amounts to the minimization of the modified E_{tv}:

$$E^a_{\text{tv}}[u] = \int_\Omega |\nabla u|_a + \frac{\lambda}{2} \int_{\Omega \setminus D} (u - u^0)^2 \, dx. \tag{4.4}$$

This energy form connects image inpainting to the classical problem of *nonparametric minimal surfaces* [48]. In fact, in the (x, y, z)–space, the first term of $E^a_{\text{tv}}[u]$, up to the multiplicative constant a, is exactly the area of the surface

$$z = z(x, y) = \frac{u(x, y)}{a}.$$

In the case when the available part u^0 is noisefree, we have

$$\lambda = \infty, \quad z\big|_{\Omega \setminus D} = z^0\big|_{\Omega \setminus D}.$$

Thus we end up with the exact minimal surface problem on the inpainting domain D:

$$\min \int_D \sqrt{1 + |\nabla z|^2} \, dx \quad \text{with } z = z^0 \text{ along } \partial D.$$

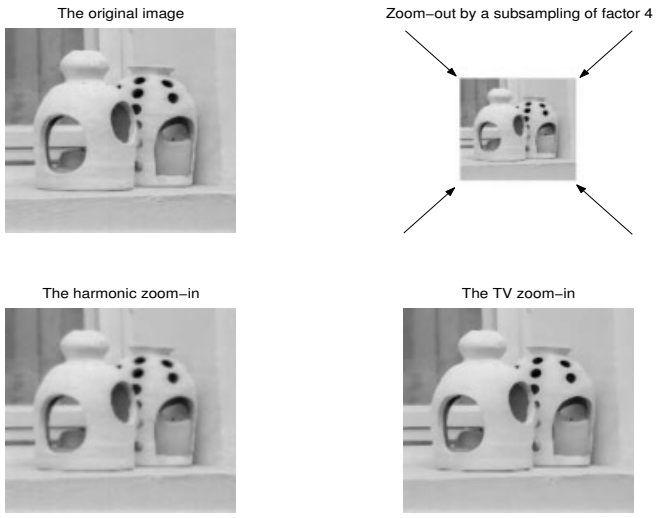

FIGURE 4.1. Digital zoom-in based on the TV inpainting scheme, as compared with that based on the harmonic inpainting scheme, i.e., that based on the Sobolev image model: $E[u] = \int_\Omega |\nabla u|^2\, dx$. Notice that the TV gives much sharper boundary reconstruction [20].

Here along the boundary, $z\big|_{\partial D}$ is understood as the trace from the interior. Since this Dirichlet problem might not be solvable for general inpainting domains D (see [48], for example), as far as inpainting is concerned, one may formulate a weaker version even for the noisefree case:

$$\min \int_D \sqrt{1 + |\nabla z|^2} + \frac{\mu}{2} \int_{\partial D} (z - z^0)^2\, d\mathcal{H}^1,$$

where μ is a large positive weight and $d\mathcal{H}^1$ the one-dimensional Hausdorff measure of ∂D. Then the existence of a minimum can be easily established based on the direct method. This is also a standard relaxation technique in the study of the minimal surface problems. An effective application of this interesting connection is for edge-based image decoding and synthesis (Figure 4.2).

Compared with all the other variational inpainting schemes, the TV model has the lowest complexity and easiest digital implementation. It works remarkably well for all *local* inpainting problems such as digital zooming (Figure 4.1), superresolution, and text removal [20]. But for large-scale problems, the TV inpainting model suffers from its origin in the length curve energy. One major drawback is its failure to realize the connectivity principle in visual perception as discussed in [21].

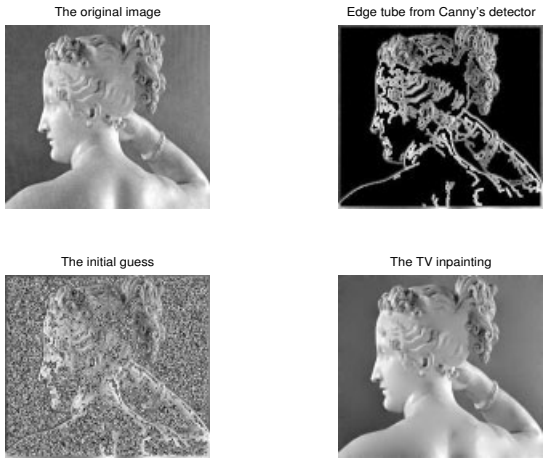

FIGURE 4.2. TV inpainting applied to the primal-sketch-based image decoding (Chan and Shen [20]).

4.2 The Elastica Inpainting

In [18], Chan, Kang, and Shen proposed to improve the TV inpainting model by using the elastica image model

$$E[u] = \int_{\Omega} (\alpha + \beta\kappa^2)|\nabla u| dx, \quad \kappa = \nabla \cdot \left[\frac{\nabla u}{|\nabla u|}\right].$$

The elastica inpainting model is thus to minimize the posterior energy

$$E_e[u \mid u^0, D] = \int_{\Omega} \phi(\kappa)|\nabla u| dx + \frac{\lambda}{2} \int_{\Omega \setminus D} (u - u^0)^2 \, dx, \tag{4.5}$$

where $\phi(s) = \alpha + \beta s^2$.

By calculus of variation, the following well-structured equation is established in [18]:

THEOREM 4.1 *Assume the images involved are regular enough so that all the high-order derivatives involved below are well-defined. Then the steepest-descent equation of the elastica energy is given in divergence form by*

$$\frac{\partial u}{\partial t} = \nabla \cdot \vec{V} + \lambda_D(x)(u^0 - u), \tag{4.6}$$

$$\vec{V} = \phi(\kappa)\vec{n} - \frac{\vec{t}}{|\nabla u|} \frac{\partial(\phi'(\kappa)|\nabla u|)}{\partial \vec{t}}. \tag{4.7}$$

Here $\vec{n}$ and $\vec{t}$ denote the normal and tangent directions:

$$\vec{n} = \frac{\nabla u}{|\nabla u|}, \quad \vec{t} = \vec{n}^{\perp}, \quad \frac{\partial}{\partial \vec{t}} = \vec{t} \cdot \nabla.$$

The natural boundary conditions along $\partial\Omega$ *with outer normals* $\vec{\nu}$ *are*

$$\frac{\partial u}{\partial \vec{\nu}} = 0 \quad \textit{and} \quad \frac{\partial(\phi'(\kappa)|\nabla u|)}{\partial \vec{\nu}} = 0.$$

Notice that the coupling between $\vec{t}$ and $\partial/\partial\vec{t}$ in (4.7) makes it safe to take any direction of $\vec{n}^{\perp}$ for $\vec{t}$.

The vector field $\vec{V}$ is called the flux of the elastica energy. Its decomposition in the natural orthogonal frame $(\vec{n}, \vec{t})$ in (4.7) has significant meaning in terms of micro-inpainting mechanisms.

(i) The normal flow $\phi(k)\vec{n}$ carries the feature of an important inpainting scheme invented earlier by Chan and Shen called CDD (*curvature driven diffusion*) [21]. CDD was discovered in the process of looking for micro mechanisms that can realize the connectivity principle in visual perception [21, 54, 75].

(ii) The tangential component can be written as

$$\vec{V}_t = -\left(\frac{1}{|\nabla u|^2}\frac{\partial(\phi'(\kappa)|\nabla u|)}{\partial \vec{t}}\right)\nabla^{\perp} u,$$

and its divergence is

$$\nabla \cdot \vec{V}_t = \nabla^{\perp} u \cdot \nabla\left(\frac{-1}{|\nabla u|^2}\frac{\partial(\phi'(\kappa)|\nabla u|)}{\partial \vec{t}}\right),$$

since $\nabla^{\perp} u$ is divergence free. Define the smoothness measure

$$L_\phi = \frac{-1}{|\nabla u|^2}\frac{\partial(\phi'(\kappa)|\nabla u|)}{\partial \vec{t}}.$$

Then the tangent component is in the form of the transport inpainting mechanism as originally invented by Bertalmio et al. [9]: $\nabla \cdot \vec{V}_t = \nabla^{\perp} u \cdot \nabla(L_\phi)$. Notice that here L_ϕ is a third-order smoothness quantity. In equilibrium when $\nabla \cdot \vec{V}_t = 0$, the smoothness measure L_ϕ has to remain constant along the level sets of u. On the inpainting domain D where image information is missing, this means that the existing information L_ϕ on $\Omega \setminus D$ is transported into D along the level sets of u. Compared with Bertalmio et al.'s practical choice of Laplacian $L = \Delta u$, we believe that L_ϕ provides a more natural and geometry-motivated "messenger."

Pure transport of Bertalmio et al. [9] can lead to shocks as is well-known in the study of conservation laws, while pure curvature-driven diffusion (CDD) of Chan and Shen [21] is only motivated by the connectivity principle in vision research and lacks theoretical support. The elastica inpainting PDE (4.6) therefore combines their strength and also offers a theoretical root.[2]

[2] Another way to stabilize Bertalmio et al.'s transport mechanism is to add viscosity, which leads to the work of Bertalmio, Bertozzi, and Sapiro on connecting inpainting to the Navier-Stokes equation in fluid dynamics [8]. On the other hand, another way to integrate the transport mechanism into Chan and Shen's CDD diffusion scheme is via an axiomatic approach as explored in [22].

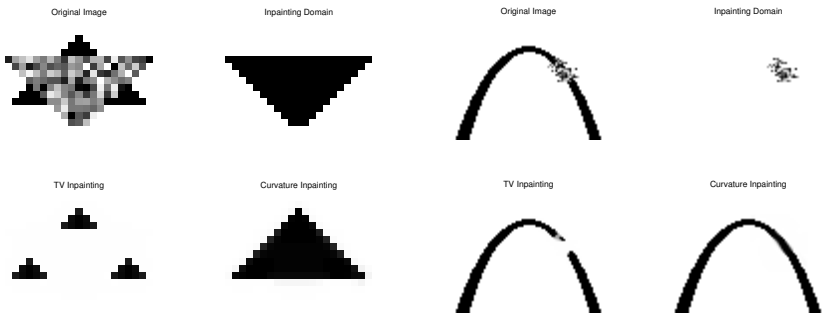

FIGURE 4.3. Two examples of elastica inpainting, as compared with TV inpainting (from Chan, Kang, and Shen [18]). In the case of large aspect ratios [21], the TV inpainting model fails to comply to the connectivity principle [21, 54, 75].

For the numerical realization of the model, we mention the following aspects. More detail can be found in [18]. Two digital examples are illustrated in Figure 4.3.

(i) To accelerate the convergence of the steepest-descent marching (4.6) toward its equilibrium solution, one can adopt the Marquina-Osher method [63] by adding a nonnegative "time correcting factor" $T = T(u, |\nabla u|)$:

$$\frac{\partial u}{\partial t} = T \cdot \big(\nabla \cdot \vec{V} + \lambda_D(x)(u^0 - u)\big).$$

For instance, take $T = |\nabla u|$. As shown in [63], such a simple technique can substantially improve the numerical marching size and speed up the convergence.

(ii) As in the TV inpainting model, for the computation of κ and $\vec{V}$, $1/|\nabla u|$ is always conditioned to $1/|\nabla u|_a$ to avoid a zero denominator. As before, $|z|_a = \sqrt{|z|^2 + a^2}$ with $a \ll 1$.

(iii) To more efficiently denoise the available image and propagate the broken edges, classical numerical techniques from computational fluid dynamics (CFD) can be very useful, including those originally designed for capturing shocks. Techniques adopted in [18] are the *upwind scheme* and the *min-mod* scheme [76].

4.3 Inpainting via the Mumford-Shah Image Model

The idea of applying the Mumford-Shah image model to inpainting and image interpolation first appeared in Tsai, Yezzi, and Willsky [88] and Chan and Shen [20], and has recently been studied again by Esedoglu and Shen [39] based on the Γ-convergence approximation theory of Ambrosio and Tortorelli [2, 3].

The model is to minimize the posterior energy

$$E_{\text{ms}}[u, \Gamma \mid u^0, D] = \frac{\gamma}{2} \int_{\Omega \setminus \Gamma} |\nabla u|^2 \, dx + \alpha \, \text{length}(\Gamma) + \frac{\lambda}{2} \int_{\Omega \setminus D} (u - u^0)^2 \, dx, \tag{4.8}$$

where γ, α, and λ are positive weights. Notice that if D is empty (i.e., there is no spatially missing domain), then the model is precisely the classical Mumford-Shah denoising and segmentation model [73]. Also, notice that unlike the previous two models, it outputs two objects: the completed and cleaned image u and its associated edge collection Γ.

Theoretically, the edge collection Γ can be any *closed* set with finite one-dimensional Hausdorff measure $\mathcal{H}^1(\Gamma)$. As a result, the more restrictive length measure in the formula should be ideally replaced by $\mathcal{H}^1(\Gamma)$. In the theoretical study of the Mumford-Shah model [1, 30, 47], a weaker form of the Mumford-Shah energy has been formulated on the so-called SBV images (special BV), for which the edge set Γ is then closely connected to the *jump set* of an SBV image.

Merely for the sake of computation, we shall now assume that Γ is sufficiently smooth (e.g., Lipschitz). For a given edge layout Γ, variation of $E_{\text{ms}}[u \mid \Gamma, u^0, D]$ gives

$$\gamma \Delta u + \lambda_D(x)(u^0 - u) = 0 \quad \text{on } \Omega \setminus \Gamma, \tag{4.9}$$

with the natural adiabatic condition $\partial u / \partial \vec{\nu} = 0$ along both Γ and $\partial\Omega$.

Denote the solution to the elliptic equation (4.9) by u_Γ. Then the steepest-descent infinitesimal move of Γ for $E_{\text{ms}}[\Gamma \mid u_\Gamma, u^0, D]$ is given by

$$\frac{dx}{dt} = \left(\alpha\kappa + \left[\frac{\gamma}{2} |\nabla u_\Gamma|^2 + \frac{\lambda_D}{2} (u_\Gamma - u^0)^2 \right]_\Gamma \right) \vec{n}. \tag{4.10}$$

Here $x \in \Gamma$ is an edge pixel and $\vec{n}$ the normal direction at x. The symbol $[g]_\Gamma$ denotes the jump of a scalar field $g(x)$ across Γ:

$$[g]_\Gamma(x) = \lim_{\sigma \to 0^+} (g(x + \sigma\vec{n}) - g(x - \sigma\vec{n})).$$

The sign of the curvature κ and the direction of the normal $\vec{n}$ are coupled so that $\kappa\vec{n}$ points to the curvature center of Γ at x.

Note that the curve evolution equation (4.10) is a combination of the *mean curvature motion* [40]

$$\frac{dx}{dt} = \alpha\kappa\vec{n}$$

and a field-driven motion specified by the second term. The field-driven motion attracts the curve toward the expected edge set, while the mean curvature motion makes sure that the curve does not develop ripples and stays smooth.

Like the TV inpainting model, the inpainting PDEs based on the Mumford-Shah image model is of second order. But the extra complexity comes from its free boundary nature. In [20, 88], the level-set method of Osher and Sethian [77] is proposed.

In the most recent work by Esedoglu and Shen [39], a simpler numerical scheme is developed based on the Γ-convergence theory of Ambrosio and Tortorelli [2, 3]. Unlike the segmentation task for which the precise edge locations are indeed an indispensable portion of the complete solution, inpainting does not really demand

the *explicit* output of the edge sets, though their implicit interpolation is still crucial. Therefore, as Esedoglu and Shen argued in [39], inpainting provides the ideal market for the application of the Γ-convergence approximation theory.

In the Γ-convergence theory, the one-dimensional edge Γ is approximately represented by its associated signature function

$$z : \Omega \to [0, 1],$$

which is close to 1 almost everywhere except on a narrow (specified by a small parameter ϵ) tubular neighborhood of Γ, where it is close to 0. The posterior energy $E_{\text{ms}}[u, \Gamma \mid u^0, D]$ is approximated by

$$\begin{aligned} E_\epsilon[u, z \mid u^0, D] = {} & \frac{1}{2}\int_\Omega \lambda_D(x)(u - u^0)^2\,dx + \frac{\gamma}{2}\int_\Omega z^2|\nabla u|^2\,dx \\ & + \alpha \int_\Omega \left(\epsilon|\nabla z|^2 + \frac{(1-z)^2}{4\epsilon}\right) dx. \end{aligned} \tag{4.11}$$

Taking variation on u and z separately yields the Euler-Lagrange system:

$$\lambda_D(x)(u - u^0) - \gamma\nabla \cdot (z^2\nabla u) = 0, \tag{4.12}$$

$$(\gamma|\nabla u|^2)z + \alpha\left(-2\epsilon\Delta z + \frac{z-1}{2\epsilon}\right) = 0, \tag{4.13}$$

with the natural adiabatic boundary conditions along $\partial\Omega$ (due to the boundary integrals coming from integration by parts):

$$\frac{\partial u}{\partial \vec{\nu}} = 0, \qquad \frac{\partial z}{\partial \vec{\nu}} = 0.$$

Define two elliptic operators acting on u and z separately:

$$L_z = -\nabla \cdot z^2\nabla + \frac{\lambda_D}{\gamma}, \tag{4.14}$$

$$M_u = \left(1 + 2\left(\epsilon\frac{\gamma}{\alpha}\right)|\nabla u|^2\right) - 4\epsilon^2\Delta. \tag{4.15}$$

Then the Euler-Lagrange system (4.12) and (4.13) can be simply written as

$$L_z u = \left(\frac{\lambda_D}{\gamma}\right)u^0 \quad \text{and} \quad M_u z = 1. \tag{4.16}$$

This coupled system can be solved easily by efficient elliptic solvers coupled with some suitable iterative schemes. Two digital examples are included in Figures 4.4 and 4.5.

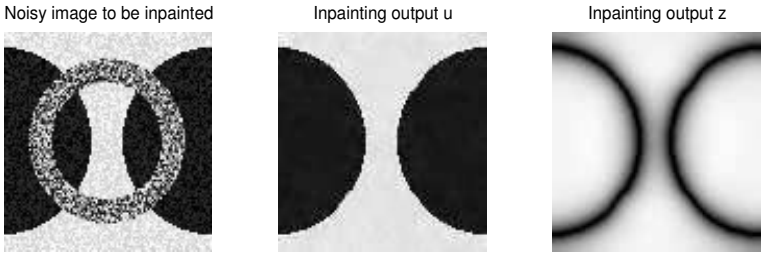

FIGURE 4.4. Inpainting based on the Γ-convergence approximation (4.11) and its associated elliptic system (4.16) (from Esedoglu and Shen [39]).

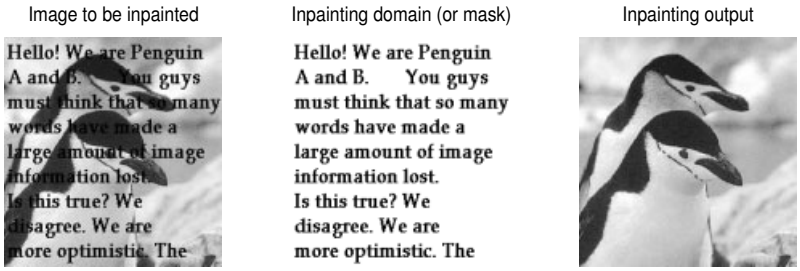

FIGURE 4.5. Text erasing by inpainting based on the Mumford-Shah image model (from Esedoglu and Shen [39]).

4.4 Inpainting via Mumford-Shah-Euler Image Model

Like the TV image model, the Mumford-Shah image model is insufficient for large-scale image inpainting problems due to the embedded length curve energy. To polish the performance of Mumford-Shah inpainting, Esedoglu and Shen [39] proposed a variational inpainting scheme based on the Mumford-Shah-Euler image model.

In this model, the posterior energy to be minimized becomes

$$E_{\text{mse}}[u, \Gamma \mid u^0, D] = \frac{\gamma}{2} \int_{\Omega \setminus \Gamma} |\nabla u|^2 \, dx + \int_{\Gamma} (\alpha + \beta \kappa^2) ds + \frac{\lambda}{2} \int_{\Omega \setminus D} (u - u^0)^2 \, dx, \tag{4.17}$$

where the length energy in E_{ms} has been upgraded to Euler's elastica energy.

As in the previous inpainting model, for a given edge layout Γ, the Euler-Lagrange equation for $E_{\text{mse}}[u \mid \Gamma, u^0, D]$ is

$$\gamma \Delta u + \lambda_D(x)(u^0 - u) = 0, \quad x \in \Omega \setminus \Gamma, \tag{4.18}$$

with the adiabatic condition along Γ and $\partial\Omega$: $\partial u/\partial\vec{\nu} = 0$.

For the solution u_Γ to this equation, the infinitesimal steepest-descent move of Γ is given by [18, 60, 69]:

$$\frac{dx}{dt} = \alpha\kappa - \beta\left(2\frac{d^2\kappa}{ds^2} + \kappa^3\right) + \left[\frac{\gamma}{2}|\nabla u_\Gamma|^2 + \frac{\lambda_D}{2}(u_\Gamma - u^0)^2\right]_\Gamma. \tag{4.19}$$

The meaning of the symbols is the same as in the preceding section.

The digital implementation of this fourth-order nonlinear evolutionary equation is highly nontrivial. The challenge lies in finding an effective numerical representation of the one-dimensional object Γ and robust ways to compute its geometry, i.e., the curvature and its differentials.

In Esedoglu and Shen [39], the equation is numerically implemented based on the Γ-convergence theory of De Giorgi [46]. As for the Mumford-Shah image model, Γ-convergence approximation leads to relatively simpler elliptic systems that can be solved efficiently in computation.

De Giorgi [46] conjectured to approximate Euler's elastica curve model

$$e(\Gamma) = \int_\Gamma (\alpha + \beta\kappa^2)ds$$

by an elliptic integral of the signature z (the two constants α and β may be different):

$$E_\epsilon[z] = \alpha \int_\Omega \left(\epsilon|\nabla z|^2 + \frac{W(z)}{4\epsilon}\right) dx + \frac{\beta}{\epsilon}\int_\Omega \left(2\epsilon\Delta z - \frac{W'(z)}{4\epsilon}\right)^2 dx, \tag{4.20}$$

where $W(z)$ can be the symmetric double-well function

$$W(z) = (1 - z^2)^2 = (z + 1)^2(z - 1)^2. \tag{4.21}$$

Unlike the choice of $W(z) = (1-z)^2$ for the Mumford-Shah image model, here the edge layout Γ is embedded as the zero level set of z. Asymptotically, as $\epsilon \to 0^+$, a boundary layer grows to realize the sharp transition between the two well states $z = 1$ and $z = -1$.

Then the original posterior energy E_{mse} on u and Γ can be replaced by an elliptic energy on u and z:

$$E_\epsilon[u, z \mid u^0, D] = \frac{\gamma}{2}\int_\Omega z^2|\nabla u|^2\, dx + E_\epsilon[z] + \frac{1}{2}\int_\Omega \lambda_D(u - u^0)^2\, dx. \tag{4.22}$$

For a given edge signature z, variation on u in $E_\epsilon[u \mid |z, u^0, D]$ gives

$$\lambda_D(u - u^0) - \gamma\nabla\cdot(z^2\nabla u) = 0, \tag{4.23}$$

with the adiabatic boundary condition $\partial u/\partial \vec{\nu} = 0$ along $\partial\Omega$. For the solution u, the steepest-descent marching of z for $E_\epsilon[z \mid |u, u^0, D]$ is given by

$$\frac{\partial z}{\partial t} = -\gamma|\nabla u|^2 z + \alpha g + \frac{\beta W''(z)}{2\epsilon^2} g - 4\beta\Delta g, \tag{4.24}$$

$$g = 2\epsilon\Delta z - \frac{W'(z)}{4\epsilon}, \tag{4.25}$$

again with the Neumann adiabatic conditions along the boundary $\partial\Omega$:

$$\frac{\partial z}{\partial \vec{\nu}} = 0 \quad \text{and} \quad \frac{\partial g}{\partial \vec{\nu}} = 0.$$

Equation (4.24) is of fourth order for z, with the leading head $-8\epsilon\beta\Delta^2 z$. Thus, to ensure stability, an explicit marching scheme would require $\Delta t = O((\Delta x)^4/\epsilon\beta)$. There are a couple of ways to stably increase the marching size. First, as inspired by Marquina and Osher [63], one can add a time-correcting factor (as in Section 4.2):

$$\frac{\partial z}{\partial t} = T(\nabla z, g \mid u)\left(-\gamma|\nabla u|^2 z + \alpha g + \frac{\beta W''(z)}{2\epsilon^2} g - 4\beta\Delta g\right),$$

where $T(\nabla z, g \mid u)$ is a suitable positive scalar, for example, $T = |\nabla z|$ [63].

The second alternative is to turn to implicit or semi-implicit schemes. Equation (4.24) can be rearranged to

$$\frac{\partial z}{\partial t} + \gamma|\nabla u|^2 z - 2\alpha\epsilon\Delta z + 8\beta\epsilon\Delta^2 z = -\frac{\alpha}{4\epsilon}W'(z) + \frac{\beta W''(z)}{2\epsilon^2} g + \frac{\beta}{\epsilon}\Delta W'(z), \tag{4.26}$$

or simply

$$\frac{\partial z}{\partial t} + L_u z = f(z),$$

where L_u denotes the positive definite elliptic operator (u-dependent)

$$L_u = \gamma|\nabla u|^2 - 2\alpha\epsilon\Delta + 8\beta\epsilon\Delta^2,$$

and $f(z)$ the entire right-hand side of (4.26). Then a semi-implicit scheme can be designed as: at each discrete time step n,

$$(1 + \Delta t L_u) z^{(n+1)} = z^{(n)} + \Delta t f(z^{(n)}),$$

where the positive definite operator $1 + \Delta t L_u$ can be numerically inverted by many fast solvers [49, 86]. A digital example is given in Figure 4.6.

5 Light Adaptivity and Weberized Variational Inpainting

Human visual perception performs remarkably well in terms of light adaptivity, which enables the vision system to maintain a stable perceptual performance in a large dynamic range of ambient light intensities from dawn to dusk. This feature has been quantitatively characterized by a celebrated law in vision psychology, psychophysics, as well as retinal physiology, known as Weber's law, named after its discoverer, German psychologist E. H. Weber [41, 91].

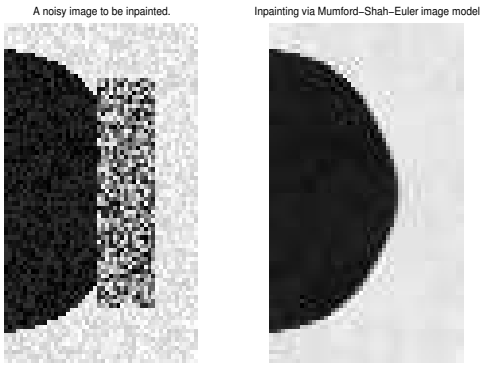

FIGURE 4.6. Inpainting based on the Mumford-Shah-Euler image model can satisfactorily restore a smooth edge as expected (from Esedoglu and Shen [39]).

In terms of regularization theory, as well explained and developed in Shen [83] and Shen and Jung [84], Weber's law implies that both the conventional Sobolev regularizer $\int_\bullet |\nabla u|^2\,dx\,dy$ (as for the cartoonish patches in the Mumford-Shah model [73]) and the TV regularizer $\int_\bullet |Du|$ should be better replaced by their Weberized versions

$$\int_\bullet \frac{|\nabla u|^2}{u^2}\,dx \quad \text{and} \quad \int_\bullet \frac{|Du|}{u}.$$

Both the theory and computational results in [83, 84] have demonstrated that such modification can faithfully simulate human vision's light adaptivity in a large dynamic range of light intensities.

Take the TV inpainting model $E_{\text{tv}}[u \mid u^0, D]$ presented in the preceding section, for example. Its Weberized version is to minimize the cost function

$$E_{\text{wtv}}[u \mid u^0, D] = \int_\Omega \frac{|Du|}{u} + \frac{\lambda}{2}\int_{\Omega\setminus D} (u-u^0)^2\,dx\,dy. \tag{5.1}$$

(The symbol D for an inpainting domain and that in $|Du|$ are unrelated, and only kept for convenience following the literature.) The images u^0 and u are understood as intensity distributions and are consequently nonnegative. On the other hand, the Weberized total variation $\int_\Omega |Du|/u$ could be understood as the real total variation of the logarithmic transform $v = \ln u$, i.e., $\int_\Omega |Dv|$.

The Weberized TV inpainting model (5.1) could similarly be solved via its formal Euler-Lagrange equation:

$$0 = -\frac{|\nabla u|}{u^2} - \nabla\cdot\left[\frac{1}{u}\frac{\nabla u}{|\nabla u|}\right] + \lambda_D(u-u^0)$$

with Neumann adiabatic condition along the boundary of Ω. The equation could be simplified to

$$0 = -\frac{1}{u}\nabla \cdot \left[\frac{\nabla u}{|\nabla u|}\right] + \lambda_D(u - u^0).$$

Or, more conveniently, define the variable weight $\Lambda_D = \Lambda_D(u) = \lambda_D \times u$. Then the Euler-Lagrange equation takes the familiar form of TV inpainting,

$$0 = -\nabla \cdot \left[\frac{\nabla u}{|\nabla u|}\right] + \Lambda_D(u)(u - u^0), \tag{5.2}$$

which can be numerically solved using some suitable iterative method with stepwise linearization, e.g., solving the following linear elliptic system for $u^{(n+1)}$ from the current best inpainting $u^{(n)}$:

$$0 = -\nabla \cdot \left[\frac{\nabla u}{|\nabla u^{(n)}|}\right] + \Lambda_D(u^{(n)})(u - u^0).$$

Proper conditioning techniques discussed in the preceding section apply here as well.

The same technique of Weberization could be applied to the Mumford-Shah inpainting as well. We refer to [83, 84] for the relevant theory and numerics related to Weber's law, light adaptivity, and the Weberization technique.

Notice also that the Weberized inpainting models are better justified in the framework of Tikhonov regularization theory than the Bayesian rationale. That is, Weber's law by its nature provides a specific way of visual regularization. It does not attempt to alter the objective image priors.

6 JPEG2000 and Variational Inpainting for Lost Wavelet Coefficients

In the wireless communication of JPEG2000 images [51], it could happen that certain wavelet packets are randomly lost during the transmission process. To recover the original images from their incomplete wavelet transforms is an inpainting problem according to the universal definition proposed in Section 2. The current section briefly outlines the recent work by Chan, Shen, and Zhou [26].

Inspired by the preceding successful variational inpainting models in the pixel domain, one may try as well to adapt for inpainting the existing variational denoising schemes in the wavelet domain. But much to one's surprise, such an attempt can only end up in failure. More specifically, we claim that the Besov image models, which are crucial in the analysis of wavelet-based denoising and compression schemes [32, 33, 34, 36], become depressingly ineffective for image inpainting with missing wavelet coefficients. For simplicity we shall only analyze the one-dimensional case, but the two-dimensional situation is essentially the same except for more involved multi-indices.

Given a regular multisolution analysis in L^2 with mother wavelet $\psi(x)$ and shape (or scaling) function $\phi(x)$ [31, 87], let $d_{jk} = d_{jk}(u)$ denote the wavelet

coefficients of a given image u:

$$u(x, y) = \sum_{j \geq -1, k} d_{jk}(u)\psi_{jk}(x),$$

where (in one dimension) for any resolution $j \geq 0$,

$$\psi_{jk}(x) = 2^{j/2}\psi(2^j x - k), \quad k \in \mathbb{Z}.$$

For notational convenience, for $j = -1$, we have set

$$\psi_{-1,k} = \phi_{0,k} = \phi(x - k), \quad k \in \mathbb{Z}.$$

As a result, $(d_{-1,k} \mid k)$ are in fact the low-pass coefficients, which are often separately denoted by $(c_{0,k} \mid k)$ in the literature.

For the least square mechanism to take effect, in addition, we assume that the multiresolution is *orthonormal* so that continuous white noises in the pixel domain are represented by discrete white noises in the wavelet domain.

THEOREM 6.1 (Insufficiency of Wavelet-Based Image Models) *Suppose*

$$E_w[u] = E_w[|d_{jk}(u)|, \ j \geq -1, \ k \in \mathbb{Z}],$$

is a type of image regularity that is monotonically increasing with respect to each argument $t_{jk} = |d_{jk}|$. Let D denote the collection of indices (j, k) for which the associated wavelet coefficients are missing, and $d^0 = (d^0_{jk} \mid (j, k) \in D^c)$ the set of available wavelet coefficients that could be degraded by stationary Gaussian white noise. Then any minimizer u^* to the variational inpainting model

$$E[u \mid d^0, D] = E_w[u] + \frac{\lambda}{2} \sum_{(j,k) \in D^c} \left(d^0_{jk} - d_{jk}(u)\right)^2$$

must satisfy

$$d^*_{jk} = d_{jk}(u^*) \equiv 0, \quad \forall (j, k) \in D.$$

We omit the proof, which is straightforward. The problem raised by the theorem is that no matter what the original wavelet coefficients are, the above variational inpainting model always restores them by filling in zeros. As a result, missing edge segments in the pixel domain are inevitably blurred due to such an action of essentially band-pass filtering.

In particular, this leads to the somewhat surprising conclusion that the *Besov image models* fail to produce meaningful inpainting models in the above variational setting, since a Besov norm in $B^\alpha_q(L^p)$ can indeed be equivalently characterized via the wavelet coefficients:

$$E_w[u] = \|u\|_{B^\alpha_q(L^p)} = \left(\sum_{j \geq -1} 2^{jq(\alpha + \frac{1}{2} - \frac{1}{p})} \|d_{j,}\|^q_{l^p} \right)^{1/q},$$

which apparently satisfies the condition of the theorem. Here $d_{j,} = (d_{jk} \mid k \in \mathbb{Z})$ denotes the sequence of wavelet coefficients at each resolution level j. (In two dimensions, the factor $\frac{1}{2} - \frac{1}{p}$ should be multiplied by 2.)

The failure of the Besov image models for inpainting is rooted in the lack of spatial correlation among wavelet coefficients, which however has been good news in the classical applications of denoising and compression. That is, wavelet representation, like the spectral decomposition of Hermitian operators, has conventionally served as the beautiful diagonalization procedure for the denoising and compression operators. But diagonalization is bad news for inpainting since interpolation demands the very opposite property—dediagonalization or coupling of information. Only via coupling can the lost information possibly be restored from what is available.

To remedy such deficiency, Chan, Shen, and Zhou [26] proposed to explicitly employ geometric image models to enforce spatial interactions between the existing and missing wavelet coefficients. Taking the BV image model, for example, one ends up with the following variational inpainting model in mixed domains, i.e., both the pixel domain and wavelet domain:

$$\min E[u \mid d^0, D] = \int_\Omega |Du| + \frac{\lambda}{2} \sum_{(j,k)\in D^c} (d^0_{jk} - d_{jk}(u))^2. \tag{6.1}$$

BV images can be approximated by Besov ones to a certain extent, but never equivalently. This is characterized by the following theorem (e.g., Meyer [66]):

THEOREM 6.2 *BV images cannot be simply characterized by the sizes of their wavelet coefficients.*

More specifically, there exists no function $\Phi = \Phi(|d_{jk}| : j \geq -1, k \in \mathbb{Z})$ such that for any $u \in \mathrm{BV}(\mathbb{R}^2)$,

$$C_1\Phi(|d_{jk}(u)| : j, k) \leq \int_\Omega |Du| \leq C_2\Phi(|d_{jk}(u)| : j, k) \tag{6.2}$$

for some $C_1, C_2 > 0$ independent of u. Here Φ is independent of the particular orthonormal wavelet basis employed, whereas C_1 and C_2 could be.

The inexistence is mainly because there exist "rotations" (i.e., unitary transforms) in $L^2(\mathbb{R}^2)$ that swing some BV images out of the BV space. This, of course, could not occur if (6.2) were valid. In fact, the remarkable works of Cohen et al. [28] and Meyer [66] show that the wavelet coefficients of a BV image sit somewhere between l^1 and weak l^1.

To conclude, unlike thresholding-based wavelet denoising schemes [16, 34, 36], the hybrid inpainting model (6.1) cannot be decoupled in the wavelet domain, which is, however, exactly what an effective inpainting model seeks.

Computationally, by noticing that

$$d_{jk}(u) = \langle u, \psi_{jk}\rangle \quad \text{and} \quad \frac{\partial d_{jk}(u)}{\partial u} = \psi_{jk},$$

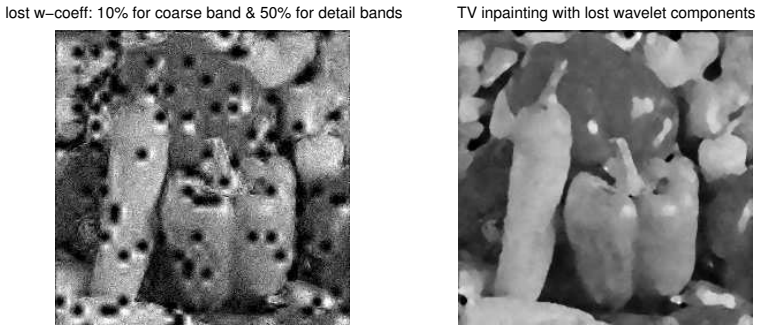

FIGURE 6.1. Output from the TV-wavelet hybrid inpainting model (6.1). Unlike in *controlled* wavelet compression schemes, wavelet components have been uncontrollably and randomly lost in all the resolutions. Due to the explicit TV control in the pixel domain, the inpainted image does not suffer the ringing effect of the Gibbs phenomenon (Chan, Shen, and Zhou [26]).

we work out the Euler-Lagrange equation for the mixed variational model (6.1):

$$0 = -\nabla \cdot \left[\frac{\nabla u}{|\nabla u|} \right] + \lambda \sum_{(j,k)\in D^c} (d_{jk}(u) - d^0_{jk})\psi_{jk}. \tag{6.3}$$

Define $T = T_D$ to be the linear *band-pass filter* in the wavelet domain:

$$T_D u = \sum_{(j,k)\in D^c} d_{jk}(u)\psi_{jk}.$$

That is, T_D is the *partial* resolution of the identity

$$T_D = \sum_{(j,k)\in D^c} |\psi_{jk}\rangle\langle\psi_{jk}|,$$

borrowing the bracket notation from quantum mechanics. In particular, T_D is nonnegative. Then the Euler-Lagrange equation can be rewritten as

$$0 = -\nabla \cdot \left[\frac{\nabla u}{|\nabla u|} \right] + \lambda T_D[u - u^0]. \tag{6.4}$$

Pay attention to the beauty shared by the new models (5.2) and (6.4) in both the current section and the previous: formally these models both look like the ordinary TV denoising model except that the Lagrange weight λ is to be upgraded to either a spatially varying function that may also depend on the image u itself or a linear operator.

For the numerical implementation and computational performance related to the hybrid model, we refer to the work by Chan, Shen, and Zhou [26]. Figure 6.1 shows the performance of the model on a test image.

7 Variational Inpainting of Meyer's Textures

In *computer graphics*, texture is almost a synonym for image, referring to any visually meaningful spatial pattern, whether regular or irregular. In image analysis and processing, though there still lacks a uniform definition, textures generally refer to those image patterns that appear to be stochastic in terms of spatial distribution (i.e., random fieldsc̆itegemgem,zhumum), oscillatory in terms of functional behavior [66], or atomic and multiscale in terms of pattern composition. Here we discuss textures in the latter sense, which is more specific.

Textures are universal in images and essential for image objects to appear real and authentic. Therefore, proper texture modeling has remained for a long while a challenging but fundamental task in image processing and analysis [44, 93, 94]. Simply put in terms of Bayesian and variational frameworks, only good texture models lead to good image processors that can effectively deal with real textures.

A comprehensive discussion on texture inpainting is outside the focus of the current paper, and in what follows we only discuss some issues related to the variational inpainting models built upon Yves Meyer's recent texture model proposed in [66].

In the context of image denoising, Meyer proposed the $u+v+w$ image model:

$$u^0(x) = u(x) + v(x) + w(x), \quad x = (x_1, x_2),$$

where u^0 denotes an observed image and the three components are

(1) the cartoonish component u, which is assumed to be BV,
(2) the texture component v, which is oscillatory and to be modeled, and
(3) the white noise component w, which is oscillatory as well but visually unattractive.

Focusing on the oscillatory behavior of textures, Meyer's new contribution is to model the texture component v by some functional spaces or spaces of generalized functions (i.e., distributions) that can properly encode oscillations. One major model is the following space of generalized functions:

$$G = \{v = \operatorname{div}(g) \mid g = (g_1, g_2) \in L^\infty(\Omega, \mathbb{R}^2)\},$$

where the divergence operator

$$\operatorname{div}(g) = \nabla \cdot g = \partial_{x_1} g_1 + \partial_{x_2} g_2$$

is in the distributional sense. That is, for any test function ϕ on the image domain Ω,

$$\langle \nabla \cdot g, \phi \rangle = -\int_\Omega g \cdot \nabla \phi \, dx.$$

The texture norm in G is defined via the minimax approach:

$$\|v\|_* = \inf \left\{ \|g\|_{L^\infty} = \sup_\Omega \sqrt{g_1^2 + g_2^2} \;\middle|\; v = \nabla \cdot g, \; g \in L^\infty(\Omega, \mathbb{R}^2) \right\}.$$

Since $L^\infty = (L^1)^*$ is a dual space, by the weak compactness of dual spaces, the norm is in fact reachable by some compatible g for any given texture $v \in G$. In addition, $\| \bullet \|_*$ is indeed a norm since the constraint $v = \nabla \cdot g$ is linear and $L^\infty(\Omega, \mathbb{R}^2)$ by itself a normed space.

For convenience, in this paper, we shall call the vector field g the *texture flow* compatible with v if $v = \nabla \cdot g$.

Under the data model $u^0 = u + v + w \in L^2$ with Gaussian white noise, a general denoising scheme based on the prior models

$$u \in \mathrm{BV} \quad \text{and} \quad v \in G$$

would be to minimize the following posterior energy:

$$E_{\mathrm{meyer}}[u, v \mid u^0] = \alpha \int_\Omega |Du| + \beta \|v\|_* + \lambda \int_\Omega (u^0 - u - v)^2 \, dx.$$

Notice that by Sobolev embedding in two dimensions, $\mathrm{BV} \subset L^2$. Thus this variational denoising model necessarily requires that the texture v belong to L^2 since both u^0 and u do. An equivalent variational formulation in terms of texture flows is given by

$$E_{\mathrm{meyer}}[u, g \mid u^0] = \alpha \int_\Omega |Du| + \beta \|g\|_\infty + \lambda \int_\Omega (u^0 - u - \nabla \cdot g)^2 \, dx.$$

Vese and Osher [89] made a p-approximation to the above energy:

$$E_{(p)}[u, g \mid u^0] = \alpha \int_\Omega |Du| + \beta \|g\|_p^p + \lambda \int_\Omega (u^0 - u - \nabla \cdot g)^2 \, dx.$$

Their numerical computation showed that in the case of denoising, even $p = 2$ already leads to some interesting results for certain classes of textures. When $p = 2$, for the energy to make sense it suffices to assume that g_1 and g_2 both belong to the Sobolev class $H^1(\Omega)$. Notice that it is *not* assumed that the texture component $v = \nabla \cdot g$ itself is Sobolev, which is apparently oversmoothing for modeling general textures.

For image and texture inpainting, the natural adaptation from the above variational model is to minimize

$$E_{(p)}[u, g \mid u^0, D] = \alpha \int_\Omega |Du| + \beta \|g\|_p^p + \lambda \int_{\Omega \setminus D} (u^0 - u - \nabla \cdot g)^2 \, dx, \tag{7.1}$$

when the image information is missing on D. Notice that the inpainting is given by $u + \nabla \cdot g$ on the entire domain.

But we claim that such a texture model lacks geometric correlation and can only lead to a trivial solution to the texture component on the missing domain. This again shows the subtle difference between denoising and inpainting.

Suppose (u^*, g^*) is a pair of minimizers to the inpainting model (7.1) on the entire image domain Ω. We claim that $g^* \equiv 0$ on the missing domain D, which makes the above variational texture inpainting less uninteresting.

First g^* must be the minimizer to the conditional energy

$$E_{(p)}[g \mid u^0, D, u^*] = \beta \int_\Omega |g|^p \, dx + \lambda \int_{\Omega \setminus D} (u^0 - u^* - \nabla \cdot g)^2 \, dx,$$

which can be written into

$$E_{(p)}[g \mid u^0, D, u^*] = \int_D \beta |g|^p \, dx + \int_{\Omega \setminus D} \left(\beta |g|^p + \lambda (u^0 - u^* - \nabla \cdot g)^2\right) dx.$$

Assume that the inpainting domain D is a closed domain and its boundary ∂D is Lipschitz-continuous, so that for any sufficiently small $\varepsilon > 0$, there exists a smooth function $\phi_\varepsilon \in [0, 1]$ on Ω that equals 1 on $\Omega \setminus D$ and 0 for any $x \in \Omega$ with $\operatorname{dist}(x, \Omega \setminus D) \geq \varepsilon$. Define $g^*_\varepsilon = \phi_\varepsilon g^*$. Then on $\Omega \setminus D$, $g^*_\varepsilon \equiv g^*$ and $\nabla \cdot g^*_\varepsilon \equiv \nabla \cdot g^*$. Since g^* is a minimizer to $E_{(p)}[g \mid u^0, D, u^*]$, one must have

$$\int_D \beta |g^*|^p \, dx \leq \int_D \beta |g^*_\varepsilon|^p \, dx = \int_D \beta |g^*|^p |\phi_\varepsilon|^p \, dx.$$

Now that $\varepsilon > 0$ is arbitrary and the right-hand side tends to 0 as $\varepsilon \to 0$, it indeed must be true that $\int_D |g^*|^p \, dx = 0$, or equivalently, $g^* \equiv 0$ on D, a.s. As a result, the inpainted texture on the missing domain $v^* = \nabla \cdot g^* = 0$, which is uninteresting and unfaithful in most applications. To summarize, we have established the following theorem:

THEOREM 7.1 *If (u^*, g^*) is a minimizer pair to the variational inpainting model (7.1), then $g^*\big|_D = 0$. That is, no interesting textures are actually filled in on the missing domain D.*

This analysis again shows that unlike the classical tasks of denoising and segmentation, texture inpainting requires image models to explicitly encode spatial or geometrical correlations. Lack of short-range or long-range correlation often fails to yield faithful reconstruction or synthesis of the missing textures from the given ones nearby. Hybridization with other texture synthesis models or algorithms (e.g., statistical synthesis) is therefore necessary for successful inpainting, as in the recent work by Bertalmio, Vese, Sapiro, and Osher [10].

8 Conclusion and Open Problems

In this expository paper, we have explored all the recent inpainting models based on the combination of the Bayesian rationale [70] and several geometric image models. Likewise, in the more classical tasks of denoising, deblurring, or segmentation, the Bayesian framework has proven very effective in designing and improving general inpainting models.

We have explained that the core ingredient for a geometric image model is the associated or embedded curve model. Based on some natural axioms such as the Euclidean and reversal invariances, we have been able to understand the general structure of geometric curve models on two-dimensional image domains. Two universal ways are discussed for "lifting" a curve model to a corresponding geometric image model.

We have shown that first-order geometric image models, such as the BV model of Rudin-Osher-Fatemi (imposed via the TV [total variation] Radon measure) [80] and Mumford-Shah model [73], function very well for classical denoising, deblurring, and segmentation problems, as well as for localized inpainting problems (such as zooming, superresolution, and text erasing) [20]. But for large-scale inpainting problems, they become inadequate for yielding perceptually meaningful outputs. Therefore, high-order geometric image models, such as the elastica model and the Mumford-Shah-Euler model, become necessary for more general inpainting applications [18, 39, 65]. The tradeoff is that high-order inpainting models are computationally much more costly and challenging.

We have described the Euler-Lagrange PDEs associated with these models, their geometric meaning as well as microscopic dynamic behavior in terms of diffusion and transport [9, 21, 22], and their digital realization based on techniques from numerical PDEs and the Γ-convergence approximation theory.

Furthermore, based on recent advances in visual perception modeling [83, 84], modeling of oscillatory patterns [66], and wireless communication of JPEG2000 images, the current paper also substantially extends the horizon of the variational inpainting literature in the last three sections.

The discussion on the inpainting of missing wavelet components and texture patches once again highlights the major difference between inpainting and all the other classical image processing tasks. That is, *spatial correlation and coupling among pixels, as encoded by lower-order geometries, are essential for any effective inpainting schemes*. We have therefore shown that both the Besov image models [32, 33, 34, 36] and Yves Meyer's recent oscillatory texture models [66] are *ineffective* image priors in the *direct* variational modeling of inpainting, though the two have performed remarkably well in the applications of denoising and compression. Other approaches to inpainting must be sought for these cases.

Though frequently referring to the Bayesian rationale, the current expository paper does not specifically address any statistical inpainting models. This will nevertheless define part of the main theme of our future work on image inpainting.

Finally, we post three interesting open problems.

(i) VIDEO INPAINTING. Video inpainting has profound application in dynamic vision analysis, surveillance analysis, and the movie industry. The first open problem is how to integrate the extra dimension of "time" into the spatial inpainting techniques and how to define geometric prior models for spatiotemporal images.

(ii) TEXTURE INPAINTING. The current work only discusses a variational inpainting model built upon Yves Meyer's recent deterministic texture models [66]. Textures more generally refer to image patterns with rich statistical features. Geometric image models can well describe the boundaries of different texture patches but are apparently insufficient for inpainting the textures themselves. Therefore, the second open problem is how to integrate geometric image models and statistical texture models and how to *grow* textures through texture synthesis without creating visually discriminable boundaries.

(iii) FAST AND EFFICIENT DIGITAL REALIZATION. Throughout this survey, numerical PDE has been a core computational tool for all the geometric inpainting models. The third open problem concerns fast and efficient digital implementation of the associated PDEs, especially for the high-order ones. There are a number of nontrivial questions to be answered, such as how to develop discretization schemes that respect geometry, the curvature, and its differentials. How to speed up convergence based on various numerical techniques such as the multigrid method and the multiresolution decomposition? Finally, the energies of high-order inpainting models, such as the elastica and the Mumford-Shah-Euler models, often have many local energy wells. It is thus another important issue to develop numerical schemes that can efficiently avoid being trapped in local energy wells, as in molecular dynamics [68].

Acknowledgments

We would like to acknowledge the support from both the Institute of Mathematics and Its Applications (IMA) at the University of Minnesota and the Institute of Pure and Applied Mathematics (IPAM) at UCLA during this project. Shen thanks Gil Strang and Stan Osher for their constant support and inspiration, as well as numerous pioneering mathematicians in MIVA (mathematical image and vision analysis) for their unique vision and insight, including Stu Geman, David Mumford, Jean-Michel Morel, and others. The authors are also profoundly grateful to our referees, who have been so constructive and creative throughout this three-year-long project and have substantially improved the quality of this final version.

Research has been supported by NSF (USA) under grant DMS-0202565 (Shen) and DMS-9973341 (Chan), and ONR under N00014-03-1-0888 (Chan).

Bibliography

[1] Ambrosio, L. A compactness theorem for a new class of functions of bounded variation. *Boll. Un. Mat. Ital. B (7)* **3** (1989), no. 4, 857–881.

[2] Ambrosio, L.; Tortorelli, V. M. Approximation of functionals depending on jumps by elliptic functionals via Γ-convergence. *Comm. Pure Appl. Math.* **43** (1990), 999–1036.

[3] Ambrosio, L.; Tortorelli, V. M. On the approximation of free discontinuity problems. *Boll. Un. Mat. Ital. B (7)* **6** (1992), no. 1, 105–123.

[4] Armstrong, S.; Kokaram, A. C.; Rayner, P. J. W. Non-linear interpolation of missing image data using minmax functions. *Proceedings of the IEEE Nonlinear Signal and Image Processing Conference, Mackinac Island, Mich. (September 1997)*. Available at: `http://www.ecn.purdue.edu/NSIP/ma35.ps`

[5] Aubert, G.; Kornprobst, P. *Mathematical problems in image processing*. Applied Mathematical Sciences, 147. New York, Springer, 2002.

[6] Ballester, C.; Bertalmio, M.; Caselles, V.; Sapiro, G.; Verdera, J. Filling-in by joint interpolation of vector fields and grey levels. *IEEE Trans. Image Process.* **10** (2001), no. 8, 1200–1211.

[7] Bellettini, G.; Dal Maso, G.; Paolini, M. Semicontinuity and relaxation properties of a curvature depending functional in 2D. *Ann. Scuola Norm. Sup. Pisa Cl. Sci. (4)* **20** (1993), no. 2, 247–297.

[8] Bertalmio, M.; Bertozzi, A. L.; Sapiro, G. Navier-Stokes, fluid dynamics, and image and video inpainting. IMA Preprint 1772, June 2001. Available at: `www.ima.umn.edu/preprints/jun01`

[9] Bertalmio, M.; Sapiro, G.; Caselles, V.; Ballester, C. *Proceedings of the 27th Annual Conference on Computer Graphics and Interactive Techniques*, 417–424. ACM Press/Addison-Wesley, New York, 2000.

[10] Bertalmio, M.; Vese, L.; Sapiro, G.; Osher, S. *Simultaneous structure and texture image inpainting*. UCLA CAM Report 02-47, July 2002.

[11] Boutin, M. Numerically invariant signature curves. *Int. J. Comp. Vision* **40** (2000), no. 3, 235–248.

[12] Brémaud, P. *Markov chains: Gibbs fields, Monte Carlo simulation, and queues*, Texts in Applied Mathematics, 31. Springer, New York, 1999.

[13] Calabi, E.; Olver, P. J.; Shakiban, C.; Tannenbaum, A.; Haker, S. Differential and numerically invariant signature curves applied to object recognition. *Int. J. Comp. Vision* **26** (1998), no. 2, 107–135.

[14] Calabi, E.; Olver, P. J.; Tannenbaum, A. Affine geometry, curve flows, and invariant numerical approximations. *Adv. Math.* **124** (1996), no. 1, 154–196.

[15] Caselles, V.; Morel, J.-M.; Sbert, C. An axiomatic approach to image interpolation. *IEEE Trans. Image Processing* **7** (1998), no. 3, 376–386.

[16] Chambolle, A.; DeVore, R. A.; Lee, N.-Y.; Lucier, B. J. Nonlinear wavelet image processing: variational problems, compression and noise removal through wavelet shrinkage. *IEEE Trans. Image Processing* **7** (1998), no. 3, 319–335.

[17] Chan, T. F.; Kang, S.-H. An error analysis on image inpainting problems. Preprint, 2004.

[18] Chan, T. F.; Kang, S.-H.; Shen, J. Euler's elastica and curvature based inpainting. *SIAM J. Appl. Math.* **63** (2002), no. 2, 564–592.

[19] Chan, T. F.; Shen, J. Variational restoration of non-flat image features: models and algorithms. *SIAM J. Appl. Math.* **61** (2000), no. 4, 1338–1361.

[20] Chan, T. F.; Shen, J. Mathematical models for local nontexture inpaintings. *SIAM J. Appl. Math.* **62** (2001), no. 3, 1019–1043.

[21] Chan, T. F.; Shen, J. Nontexture inpainting by curvature driven diffusions (CDD). *J. Visual Comm. Image Rep.* **12** (2001), no. 4, 436–449.

[22] Chan, T. F.; Shen, J. Inpainting based on nonlinear transport and diffusion. *Inverse problems, image analysis, and medical imaging: AMS Special Session on Interaction of Inverse Problems and Image Analysis, January 10–13, 2001, New Orleans, Louisiana*, 53–65. Edited by M. Z. Nashed and O. Scherzer. American Mathematical Society, Providence, R.I., 2002.

[23] Chan, T. F.; Shen, J. On the role of the BV image model in image restoration. *Recent advances in scientific computing and partial differential equations: International Conference on the Occasion of Stanley Osher's 60th Birthday, December 12–15, 2002, Hong Kong Baptist*

University, Hong Kong, 330. Edited by S. Y. Cheng, C.-W. Shu, and T. Tang. Contemporary Mathematics, 330. American Mathematical Society, Providence, R.I., 2003.

[24] Chan, T. F.; Shen, J. *Image analysis and processing: variational, pde, wavelets, and stochastic methods*. SIAM, Philadelphia, in press.

[25] Chan, T. F.; Shen, J.; Vese, L. Variational PDE models in image processing. *Notices Amer. Math. Soc.* **50** (2003), no. 1, 14–26.

[26] Chan, T. F.; Shen, J.; Zhou, H.-M. *Total variation wavelet inpainting*. UCLA CAM Report 04-47, July 2004.

[27] Chanas, L.; Cocquerez, J. P.; Blanc-Talon, J. Highly degraded sequences restoration and inpainting. Preprint, 2001.

[28] Cohen, A.; DeVore, R.; Petrushev, P.; Xu, H. Nonlinear approximation and the space $\mathrm{BV}(R^2)$. *Amer. J. Math.* **121** (1999), no. 3, 587–628.

[29] Cover, T. M.; Thomas, J. A. *Elements of information theory*. Wiley, New York, 1991.

[30] Dal Maso, G.; Morel, J.-M.; Solimini, S. A variational method in image segmentation: existence and approximation results. *Acta. Math.* **168** (1992), no. 1-2, 89–151.

[31] Daubechies, I. *Ten lectures on wavelets*. SIAM, Philadelphia, 1992.

[32] DeVore, R. A.; Jawerth, B.; Lucier, B. J. Image compression through wavelet transform coding. *IEEE Trans. Information Theory* **38** (1992), no. 2, 719–746.

[33] DeVore, R. A.; Jawerth, B.; Popov, V. Compression of wavelet coefficients. *Amer. J. Math.* **114** (1992), 737–785.

[34] Donoho, D. L. De-noising by soft-thresholding. *IEEE Trans. Information Theory* **41** (1995), no. 3, 613–627.

[35] Donoho, D. L.; Huo, X. Beamlets and multiscale image analysis. *Multiscale and multiresolution methods*, 149–196. Springer, Berlin, 2002.

[36] Donoho, D. L.; Johnstone, I. M. Ideal spacial adaption by wavelet shrinkage. *Biometrika* **81** (1994), 425–455.

[37] Elder, J. H.; Goldberg, R. M. Image editing in the contour domain. *1998 Conference on Computer Vision and Pattern Recognition (CVPR '98), June 23–25, 1998, Santa Barbara, CA, USA*, 374–381. IEEE Computer Society, Los Alamitos, Calif., 1998.

[38] Emile-Male, G. *The restorer's handbook of easel painting*. Van Nostrand Reinhold, New York, 1976.

[39] Esedoglu, S.; Shen, J. Digital inpainting based on the Mumford-Shah-Euler image model. *European J. Appl. Math.* **13** (2002), 353–370.

[40] Evans, L. C.; Spruck, J. Motion of level sets by mean curvature. I. *J. Differential Geom.* **33** (1991), no. 3, 635–681.

[41] Fechner, G. T. Über ein wichtiges psychophysiches Grundgesetz und dessen Beziehung zur Schäzung der Sterngrössen. Abk. k. Ges. Wissensch. *Math.-Phys.* **K1, 4** (1858).

[42] Fleming, W. H.; Rishel, R. An integral formula for total gradient variation. *Arch. Math.* **11** (1960), 218–222.

[43] Freeman, H. On the encoding of arbitrary geometric configuration. *IRE Transactions on Electronic Computers* **EC-10(2)** (1961), 260–268.

[44] Geman, S.; Geman, D. Stochastic relaxation, Gibbs distributions, and the Bayesian restoration of images. *IEEE Trans. Pattern Anal. Machine Intell.* **6** (1984), 721–741.

[45] Gibbs, W. *Elementary principles of statistical mechanics*. Yale University Press, New Haven, Conn., 1902.

[46] De Giorgi, E. Frontiere orientate di misura minima. *Seminario di Matematica della Scuola Normale Superiore di Pisa, 1960–61*. Editrice Tecnico Scientifica, Pisa, 1961.

[47] De Giorgi, E.; Carriero, M.; Leaci, A. Existence theorem for a minimum problem with free discontinuity set. *Arch. Rational Mech. Anal.* **108** (1989), no. 3, 195–218.

[48] Giusti, E. *Minimal surfaces and functions of bounded variation*. Birkhäuser, Boston, 1984.

[49] Golub, G. H.; Ortega, J. M. *Scientific computing and differential equations. An introduction to numerical methods*. Academic Press, Boston, 1992.

[50] Igehy, H.; Pereira, L. Image replacement through texture synthesis. *Proceedings of the 1997 International Conference on Image Processing (ICIP '97), Washington, D.C., October 26-29, 1997*, vol. 3, 186–189. IEEE Computer Society, 1997. Available at:
`http://computer.org/proceedings/icip/8183/index.htm`

[51] ISO/IEC 15444-1:2000. Information technology–JPEG 2000 image coding system. Part 1: Core coding system.

[52] Jung, K.-H.; Chang, J.-H.; Lee, C. W. Error concealment technique using data for block-based image coding. *SPIE* **2308** (1994), 1466–1477.

[53] Kang, S.-H.; Chan, T.-F.; Soatto, S. *Landmark based inpainting from multiple views*. UCLA CAM Report 02-11, March 2002.

[54] Kanizsa, G. *Organization in vision*. Praeger, New York, 1979.

[55] Karatzas, I.; Shreve, S. E. *Brownian motion and stochastic calculus*. Springer, New York, 1997.

[56] Knill, D. C.; Richards, W. *Perception as Bayesian inference*. Cambridge University Press, Cambridge–New York, 1996.

[57] Kokaram, A. C.; Morris, R. D.; Fitzgerald, W. J.; Rayner, P. J. W. Detection of missing data in image sequences. *IEEE Trans. Image Process.* **11** (1995), no. 4, 1496–1508.

[58] Kokaram, A. C.; Morris, R. D.; Fitzgerald, W. J.; Rayner, P. J. W. Interpolation of missing data in image sequences. *IEEE Trans. Image Process.* **11** (1995), no. 4, 1509–1519.

[59] Kwok, W.; Sun, H. Multidirectional interpolation for spatial error concealment. *IEEE Trans. Consumer Electronics* **39** (1993), no. 3, 455–460.

[60] Langer, J.; Singer, D. A. The total squared curvature of closed curves. *J. Diff. Geom.* **20** (1984), no. 1, 1–22.

[61] Malgouyres, F. *Increase in the resolution of digital images: Variational theory and applications*. Doctoral dissertation, Ecole Normale Supérieure de Cachan, Cachan, France, 2000.

[62] Malgouyres, F.; Guichard, F. Edge direction preserving image zooming: A mathematical and numerical analysis. *SIAM J. Numer. Anal.* **39** (2001), no. 1, 1–37.

[63] Marquina, A.; Osher, S. Explicit algorithms for a new time dependent model based on level set motion for nonlinear deblurring and noise removal. *SIAM J. Sci. Comput.* **22** (2000), no. 2, 387–405.

[64] Marr, D.; Hildreth, E. Theory of edge detection. *Proc. Royal Soc. London* **B207** (1980): 187–217.

[65] Masnou, S.; Morel. J.-M. Level-lines based disocclusion. *Proceedings of the 1998 IEEE International Conference on Image Processing (ICIP-98), Chicago, Illinois, October 4-7, 1998*, vol. 3, 259–263. IEEE Computer Society, 1998.

[66] Meyer, Y. *Oscillating patterns in image processing and nonlinear evolution equations*. University Lecture Series, 22. American Mathematical Society, Providence, R.I., 2001.

[67] Milnor, J. W. *Topology from the differentiable viewpoint*. Rev. ed. Princeton University Press, Princeton, N.J., 1997.

[68] Moré, J. J.; Wu, Z. Issues in large-scale global molecular optimization. *Large-scale optimization with applications*, 99–121. Edited by L. T. Biegler et al. Springer, New York, 1997.

[69] Mumford, D. Elastica and computer vision. *Algebraic geometry and its applications*, 491–506. Edited by C. L. Bajaj. Springer, New York, 1994.

[70] Mumford, D. The Bayesian rationale for energy functionals. *Geometry-driven diffusion in computer vision*, 141–153. Edited by B. M. ter Haar Romeny. Kluwer Academic, Boston, 1994.

[71] Mumford, D. Pattern theory: the mathematics of perception. *Proceedings of the International Congress of Mathematicians, Vol. I (Beijing, 2002)*, 401–422. Higher Education Press, Beijing, 2002.

[72] Mumford, D.; Gidas, B. Stochastic models for generic images. *Quart. Appl. Math.* **59** (2001), no. 1, 85–111.

[73] Mumford, D.; Shah, J. Optimal approximations by piecewise smooth functions and associated variational problems. *Comm. Pure Appl. Math.* **42** (1989), no. 5, 577–685.

[74] Nitsche, J. C. C. *Lectures on minimal surfaces*. Cambridge University Press, Cambridge–New York, 1989.

[75] Nitzberg, M.; Mumford, D.; Shiota, T. *Filtering, segmentation, and depth*. Lecture Notes in Computer Science, 662. Springer, Berlin–New York, 1993.

[76] Osher, S.; Rudin, L. Feature-oriented image enhancement using shock filters. *SIAM J. Numer. Anal.* **27** (1990), no. 4, 919–940.

[77] Osher, S.; Sethian, J. A. Fronts propagating with curvature-dependent speed: algorithms based on Hamilton-Jacobi formulations. *J. Comput. Phys.* **79** (1988), no. 1, 12–49.

[78] Perona, P.; Malik, J. Scale-space and edge detection using anisotropic diffusion. *IEEE Trans. Pattern Anal. Machine Intell.* **12** (1990), 629–639.

[79] Rudin, L.; Osher, S. Total variation based image restoration with free local constraints. *Proceedings of the 1994 International Conference on Image Processing (ICIP '94) Austin, Texas, USA, November 13-16, 1994*, vol. 1, 31-35. IEEE Computer Society.

[80] Rudin, L.; Osher, S.; Fatemi, E. Nonlinear total variation based noise removal algorithms. *Phys. D* **60** (1992), 259–268.

[81] Sapiro, G. *Geometric partial differential equations and image analysis*. Cambridge University Press, Cambridge, 2001.

[82] Shen, J. Inpainting and the fundamental problem of image processing. *SIAM News* **36** (2003), no. 5.

[83] Shen, J. On the foundations of vision modeling I. Weber's law and Weberized TV restoration. *Phys. D* **175** (2003), 241–251.

[84] Shen, J.; Jung, Y.-M. *On the foundations of vision modeling IV. Weberized Mumford-Shah model with Bose-Einstein noise: light adapted segmentation inspired by vision psychology, retinal physiology, and quantum statistics*. UCLA CAM Report 03-74, December 2003.

[85] Smale, S.; Zhou, D.-X. Shannon sampling and function reconstruction from point values. *Bull. Amer. Math. Soc. (N.S)* **41** (2004), no. 3, 279–305.

[86] Strang, G. *Introduction to applied mathematics*. Wellesley-Cambridge Press, Wellesley, Mass., 1986.

[87] Strang, G.; Nguyen, T. *Wavelets and filter banks*. Wellesley-Cambridge Press, Wellesley, Mass., 1996.

[88] Tsai, A.; A. Yezzi, J.; Willsky, A. S. Curve evolution implementation of the Mumford-Shah functional for image segmentation, denoising, interpolation, and magnification. *IEEE Trans. Image Process.* **10** (2001), no. 8, 1169–1186.

[89] Vese, L. A.; Osher, S. J. *Modeling textures with total variation minimization and oscillating patterns in image processing*. UCLA CAM Report 02-19, May 2002.

[90] Walden, S. *The ravished image*. St. Martin's Press, New York, 1985.

[91] Weber, E. H. De pulsu, resorptione, audita et tactu. *Annotationes anatomicae et physiologicae*. Koehler, Leipzig, 1834.

[92] Wei, L.-Y.; Levoy, M. Fast texture synthesis using tree-structured vector quantization. *Proceedings of the 27th Annual Conference on Computer Graphics and Interactive Techniques*, 479–488. ACM Press/Addison-Wesley, New York, 2000.

[93] Zhu, S. C.; Mumford, D. Prior learning and Gibbs reaction-diffusion. *IEEE Trans. Pattern Anal. Machine Intell.* **19** (1997), no. 11, 1236–1250.

[94] Zhu, S. C.; Wu, Y. N.; Mumford, D. Minimax entropy principle and its applications to texture modeling. *Neural Computation* **9** (1997), 1627–1660.

TONY F. CHAN
Department of Mathematics
University of California, Los Angeles
Los Angeles, CA 90095
E-mail: TonyC@college.ucla.edu

JIANHONG (JACKIE) SHEN
School of Mathematics
University of Minnesota
Minneapolis, MN 55455
E-mail: jhshen@math.umn.edu

Received January 2002.
Revised October 2004.